

AD-A191 135

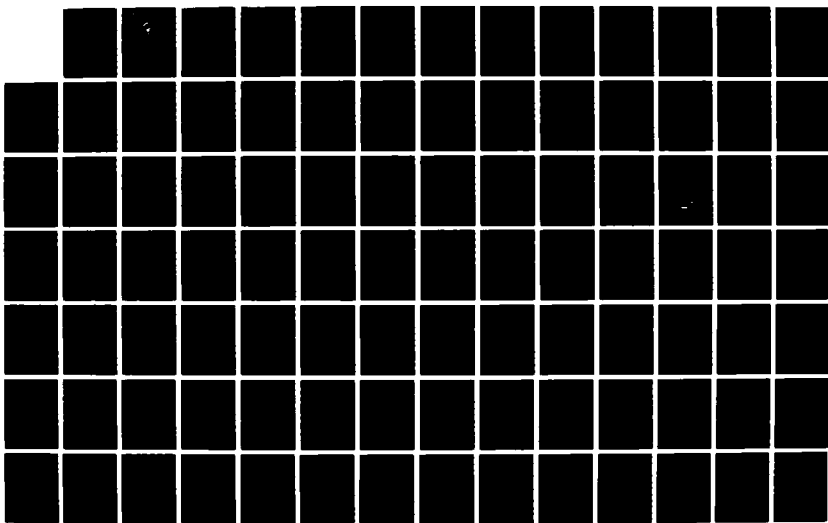
SKY RADIANCE DISTRIBUTIONS FOR THERMAL IMAGING  
BACKGROUNDS(U) NAVAL POSTGRADUATE SCHOOL MONTEREY CA  
A KOTSIS DEC 87

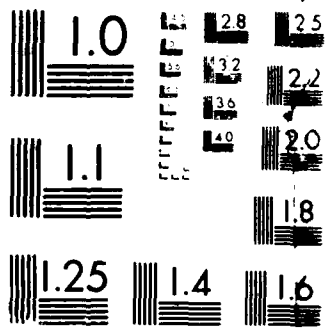
1/2

UNCLASSIFIED

F/G 4/1

NL





AD-A191 135

DTIC FILE COPY (2)

# NAVAL POSTGRADUATE SCHOOL

Monterey, California



DTIC  
ELECTE  
MAR 28 1988  
S H D

## THESIS

SKY RADIANCE DISTRIBUTIONS  
FOR  
THERMAL IMAGING BACKGROUNDS

by

Apostolos Kotsis

December 1987

Thesis Advisors:

A.W. Cooper  
and  
J. Powers

Approved for public release; distribution is unlimited

88 3 22 051

# REPORT DOCUMENTATION PAGE

1a. REPORT SECURITY CLASSIFICATION <b>UNCLASSIFIED</b>			1b. RESTRICTIVE MARKINGS		
2a. SECURITY CLASSIFICATION AUTHORITY			3. DISTRIBUTION / AVAILABILITY OF REPORT <b>Approved for public release; distribution is unlimited</b>		
2b. DECLASSIFICATION / DOWNGRADING SCHEDULE					
4. PERFORMING ORGANIZATION REPORT NUMBER(S)			5. MONITORING ORGANIZATION REPORT NUMBER(S)		
6a. NAME OF PERFORMING ORGANIZATION <b>Naval Postgraduate School</b>		6b. OFFICE SYMBOL (If applicable) <b>61</b>	7a. NAME OF MONITORING ORGANIZATION <b>Naval Postgraduate School</b>		
6c. ADDRESS (City, State, and ZIP Code) <b>Monterey, California 93943-5000</b>			7b. ADDRESS (City, State, and ZIP Code) <b>Monterey, California 93943-5000</b>		
8a. NAME OF FUNDING / SPONSORING ORGANIZATION		8b. OFFICE SYMBOL (If applicable)	9. PROCUREMENT INSTRUMENT IDENTIFICATION NUMBER		
8c. ADDRESS (City, State, and ZIP Code)			10. SOURCE OF FUNDING NUMBERS		
			PROGRAM ELEMENT NO.	PROJECT NO.	TASK NO.
					WORK UNIT ACCESSION NO.
11. TITLE (Include Security Classification) <b>SKY RADIANCE DISTRIBUTIONS FOR THERMAL IMAGING BACKGROUNDS</b>					
12. PERSONAL AUTHOR(S) <b>Kotsis, Apostolos</b>					
13a. TYPE OF REPORT <b>Master's Thesis</b>		13b. TIME COVERED FROM _____ TO _____		14. DATE OF REPORT (Year, Month, Day) <b>1987 December</b>	
15. PAGE COUNT <b>137</b>					
16. SUPPLEMENTARY NOTATION <i>Flow</i>					
17. COSATI CODES			18. SUBJECT TERMS (Continue on reverse if necessary and identify by block number)		
FIELD	GROUP	SUB-GROUP	→ <b>Background Radiation, Radiation Measurements</b>		
			<b>BMAP Analysis, Infrared Data Transfer.</b>		
19. ABSTRACT (Continue on reverse if necessary and identify by block number)					
<p>→ <b>The Background Measurements and Analysis program (BMAP) operated mostly by Naval Surface Weapons Center (NSWC) is a program of measurement and analysis of background scenes appropriate to generic infrared imaging systems.</b></p> <p><b>A computer code generated under contract, for this program, has been made available to NACIT (Naval Academic Center for Infrared Technology), at Naval Postgraduate School (NPS) by NSWC. This code includes two stored measurement data sets for 2 dimensional Fast Fourier Transform comparison and other processing techniques, a version of LOWTRAN propagation code and high resolution graphics. This work is the evaluation of this code for use to provide test data sets to</b></p>					
20. DISTRIBUTION / AVAILABILITY OF ABSTRACT <input type="checkbox"/> UNCLASSIFIED/UNLIMITED <input type="checkbox"/> SAME AS RPT <input type="checkbox"/> DTIC USERS			21. ABSTRACT SECURITY CLASSIFICATION <b>Unclassified</b>		
22a. NAME OF RESPONSIBLE INDIVIDUAL <b>A. W. Cooper</b>			22b. TELEPHONE (Include Area Code) <b>(408) 646 2452</b>		22c. OFFICE SYMBOL <b>61Cr</b>

the IRSTD data processing/acquisition system, the evaluation of AGA DISCO program for use with the BMAP, the evaluation of the present IRSTD/MASSCOMP system for use with the BMAP and the transfer of the extracted BMAP data sets, obtained during an experiment conducted mid-September 1984 at the Raytheon company location, at Bedford MA, to the Masscomp computer of the IRSTD system in IRSTD data form. *Raytheon - 11-11-84*

Approved for public release; distribution is unlimited

Sky Radiance Distributions  
for  
Thermal Image Backgrounds

by

Apostolos Kotsis  
Lieutenant, Hellenic Navy  
B.S., Hellenic Naval Academy, 1979

Submitted in Partial fulfillment of the  
requirements for the degrees of

MASTER OF SCIENCE IN PHYSICS


and

MASTER OF SCIENCE IN ENGINEERING SCIENCE


from the

NAVAL POSTGRADUATE SCHOOL  
December 1987


Author:


  
Apostolos Kotsis


Approved by:

  
A.W. Cooper, Thesis Advisor

  
J.P. Powers, Coadvisor

  
K.E. Woehler, Chairman  
Department of Physics

  
J.P. Powers, Chairman  
Department of Electrical and  
Computer Engineering

  
Gordon E. Schacher  
Dean of Science and Engineering

## ABSTRACT

The Background Measurements and Analysis program (BMAP) operated mostly by Naval Surface Weapons Center (NSWC) is a program of measurement and analysis of background scenes appropriate to generic infrared imaging systems.

A computer code generated under contract, for this program, has been made available to NACIT (Naval Academic Center for Infrared Technology) at Naval Postgraduate School (NPS) by NSWC. This code includes two stored measurement data sets for 2 dimensional Fast Fourier Transform comparison and other processing techniques, a version of LOWTRAN propagation code and high resolution graphics. This work is the evaluation of this code for use to provide test data sets to the IRSTD data processing/acquisition system, the evaluation of AGA DISCO program for use with the BMAP, the evaluation of the present IRSTD/MASSCOMP system for use with the BMAP and the transfer of the extracted BMAP data sets, obtained during an experiment conducted mid-September 1984 at the Raytheon company location, at Bedford MA, to the Masscomp computer of the IRSTD system in IRSTD data form.

## TABLE OF CONTENTS

I. INTRODUCTION.....	13
II. THE BACKGROUND PROBLEM.....	19
A. BACKGROUND AND TARGETS.....	19
B. SPATIAL AND BACKGROUND RADIANCE (NOISE).....	19
C. TARGET-BACKGROUND BRIGHTNESS/TEMPERATURE DIFFERENCE.....	21
D. SPECTRAL-SPATIAL DISCRIMINATION (CLUTTER SUPPRESSION).....	27
E. WIENER SPECTRUM / POWER SPECTRAL DENSITY.....	29
F. MONTE CARLO SCATTERING.....	33
III. RADIANCE IN THE BACKGROUND PROBLEM.....	37
A. SPECTRAL RADIANCE OF THE SKY.....	37
1. Introduction.....	37
2. Scattering.....	37
3. Emission of Atmospheric Particles.....	39
B. SPECTRAL RADIANCE ABOVE 3 $\mu$ m-CLEAR SKY.....	41
C. CLOUD RADIANCE.....	45
D. RADIATION OF AN OVERCAST SKY.....	48
E. MARINE BACKGROUND RADIANCES.....	50
1. Introduction.....	50
2. Material Properties of the Bottom.....	50
3. Temperature Distribution of the Surface.....	51





4. Optical Properties of Sea Water.....	52
5. Wave Slope Distribution and Surface Geometry...	53
IV. THE BACKGROUND MEASUREMENTS AND ANALYSIS PROGRAM.....	56
A. GENERAL.....	56
1. Introduction.....	56
2. Model Parameters (Present Version of BMAP).....	57
3. Computer Model for the Cloud Radiance.....	59
B. CODE DEVELOPMENT.....	60
C. LOWTRANS PROGRAM.....	62
V. COMPUTER CODE FOR CLUTTER - KEY FUNCTIONS.....	66
A. GENERAL.....	66
B. COMPUTER MODULES.....	68
1. Display Module.....	68
2. Analysis Module.....	74
3. Modeling Module.....	77
VI. BMAP TAPE FORMAT.....	80
A. GENERAL.....	80
B. INTERNAL CONFIGURATION.....	80
1. Introduction.....	80
2. Structure of "Header 1".....	84
3. Structure of "Header 2".....	85
4. Data Structure.....	88
5. Physical Interpretation of the data.....	90

VII. AGA DATA FORMAT.....	92
A. GENERAL.....	92
B. IMAGE/DATA TRANSFER.....	92
VIII. DATA PROCESSING IN THE IRSTD SYSTEM.....	96
A. GENERAL.....	96
B. INTERNAL CONFIGURATION OF THE IRSTD.....	96
1. Signal Processing Subsystem.....	96
2. Data Processor Subsystem.....	99
3. Display and Control Subsystem.....	100
4. Data Processing.....	100
C. DATA INPUT CONFIGURATION.....	101
1. Introduction.....	101
2. Synchronization and Geometry of the Data.....	102
IX. DATA ANALYSIS.....	106
A. GENERAL.....	106
B. COMPUTER CODE ANALYSIS.....	106
1. Introduction.....	106
2. Code analysis.....	108
X. CONCLUSIONS AND RECOMMENDATIONS.....	112
A. CONCLUSIONS.....	112
B. RECOMMENDATIONS.....	114

APPENDIX A:	LOWTRAN (LOWIN-LOWPLOT) INPUT FILES.....	116
APPENDIX B:	COMPUTER CODE IN RM/FORTRAN TO EXTRACT THE DATA FROM THE BEDFORD FILES OF THE BMAP.....	118
APPENDIX C:	KEY FUNCTIONS FOR THE BMAP PROGRAM.....	123
APPENDIX D:	COMPUTER CODE SUPPLIED BY ONTAR COMPANY TO READ THE BEDFORD FILES FROM THE BMAP.....	131
LIST OF REFERENCES.....		132
INITIAL DISTRIBUTION LIST.....		136

## LIST OF FIGURES

2.1	Background brightness versus threshold contrast....	22
2.2	Radiation contrast for the 3.5 to 5 $\mu\text{m}$ band.....	25
2.3	Radiation contrast for the 8 to 14 $\mu\text{m}$ band.....	25
2.4	Target acquisition range as a function of target to background temperature difference.....	26
2.5	Target classification and identification ranges as a function of target to background temperature difference.....	27
2.6	Techniques for measuring Wiener Spectra.....	31
3.1	Scattering patterns.....	37
3.2	Spectral radiance of the sky in a idealized form...	40
3.3	Spectral radiance of a clear night sky at Colorado.	42
3.4	Spectral radiance of a clear sky at Florida.....	43
3.5	Comparison of spectral radiances for various temperatures in Colorado.....	44
3.6	Thermal radiation through clouds.....	46
3.7	Spectral radiance of a dark cumulus cloud.....	48
3.8	Spectral radiance for high altitudes.....	48
3.9	Spectral emissivity of cloud layers thickness $\delta z$ ...	49
3.10	Spectral emissivity of cloud layers thickness $\delta z$ ...	50
3.11	Thermal structure of the sea boundary layer.....	53
3.12	Reflection of sea water surface at 0°, 60° and 80° angle of incidence.....	54
3.13	Reflectance and emissivity of water vs incidence...	54

3.14	Incidences of refraction of sea water calculated from refractivity data.....	55
3.15	Reflection of solar radiation from a flat and from a rough sea surface.....	55
4.1	Structural outline of the BMAP program.....	62
4.2	Various atmospheric models in use with the LOWTRAN6 code.....	63
5.1	Summary of DISPLAY, ANALYSIS and MODELING modules..	67
5.2	Two dimensional plot for channel #3 for BEDFORD1...	70
5.3	Two dimensional plot for channel #6 for BEDFORD1...	71
5.4	Three dimensional plot of BEDFORD1 file (all 16 channels).....	73
5.5	Two dimensional plot of BEDFORD1 file for power spectrum.....	75
6.1	BEDFORD files byte structure.....	82
6.2	BEDFORD files "HEADER 1" configuration.....	83
6.3	BEDFORD files "HEADER 2" configuration.....	85
6.4	Complex format for image data.....	89
6.5	Multi-channel data storing method.....	89
6.6	Data structure format of BEDFORD files.....	90
7.1	REDA subroutine directory configuration.....	94
8.1	Signal processing Subsystem layout #1.....	97
8.2	Signal processing Subsystem layout #2.....	98
8.3	Format of the 16 bits words input to DCU.....	101
8.4	Data matrix for 180 sensors of the optical unit...	103
8.5	Transfer of data in the Masscomp computer.....	105

9.1	Formatted Sequential data.....	108
9.2	DOS data SWAP for Integer*2 data.....	110
9.3	BMAP data SWAP for Integer*2 data.....	110

### ACKNOWLEDGEMENTS

The author of this thesis would like to express his sincere appreciation to Jerry Lentz whose help in creating the Fortran program used in this thesis was a major assistance.

I would also like to express my appreciation to Professor Cooper (whom I was continuously disturbing during the creation of this thesis) for his patience and his guidance.

The guidance of Professor Powers, with his advice assured the proper completion of this work and his help is greatly appreciated.

## I. INTRODUCTION

By the term "Remote Sensing" we mean the procedure by which one can get information about a target and its environment with the use of a sensor which is not actually in contact with the object under study.

In our modern era one of the most important methods for surveillance and tracking of targets is infrared (IR) technology. Infrared technology consists of devices whose information depends upon the electromagnetic radiation of wavelengths between 0.7 and 1000 micrometers ( $0.7$  to  $1000 \times 10^{-4}$  cm) which is absorbed by, reflected from, or emitted by different objects. By using the natural emission from objects most infrared systems can be used as detectors or target designators. Since infrared systems are passive the advantages of such systems are enormous.

But as for all systems the infrared systems have their limitations. Particle effects on transmission through clouds and fog limiting the performance of the infrared radiation almost as much as the visible radiation, although the infrared can penetrate the atmospheric haze more effectively than the visible light because of its longer wavelength. The various atmospheric gases absorb at several wavelengths of the infrared region leaving some areas where radiation can be effectively transmitted, known as atmospheric windows.



Since all targets which have a temperature above absolute zero radiate energy there is always a certain amount of radiation from the background present that must be contended with for the detection of a weak or a distant target. The reflected sunlight in the near infrared region ( $< 3$  micrometers) represents an important problem in the detection of a target (aircraft) against a cloud background at daytime.

The above factors imply that a detection and surveillance infrared system will have a limited all-weather or daytime capability unless some techniques are brought to bear which will discriminate the target from the background.

For the development of such a system it is important to specify the infrared radiance for an earth's atmospheric scene. What is also required is the full knowledge of the spatial and spectral structure of the background as well as the atmospheric effects on the emitted thermal radiation and intensity of the target.

The radiation reflected or emitted from the target mixes with the radiation from the surrounding objects and creates confusion for a detection and surveillance system. Surrounding objects may include clouds, buildings, land etc which reflect radiation from the sun or emit radiation of their own. The sea radiance which is largely due to the sun/sky radiation reflected by the sea must also be taken into consideration in designing a system for target detection for low angles above the sea water (ships or low flying

airplanes). Most systems for detection and recognition depend on the "Radiance Contrast" described by the "Temperature Difference" between the target and the background. It must be noted that the "Temperature Difference" can be deceptive, in the case of the radiance contrast, unless the reflected radiation is also considered.

For thermal imaging systems the background scene's radiance is usually suppressed. That suppression allows the creation of high image contrasts.

A good detection and surveillance system can be created only if magnitudes and variations in the radiance from different background scenes have been studied and taken into account with the infrared target appearing in them.

At the present time NACIT is developing an Infrared Search and Target Designation System (IRSTD) modified from the original ADM version of the AN/SAR-8 (IRST) which will provide threat warning and target track information. One of the potential problems for the IRSTD is the false alarms that may result from the presence of clouds and sea clutter in the environment of the target. It is important to understand that an infrared sensing system will try to detect the infrared radiance in a specific field of view (FOV) requiring high spatial resolution data. For this reason NSWC and Naval Research Laboratories (NRL) in support of the Naval requirements for fleet defense systems created a computer program for an IBM/AT micro computer called the NSWC Clutter

Measurements Code which was further supported by the Background Measurement and Analysis Program (BMAP) for the analysis of background scenes appropriate to generic infrared systems. A copy of that code, generated by ONTAR Corporation under contract, was made available to NACIT. This code includes three stored measurement data sets, other processing techniques, a version of the LOWTRAN propagation code and a high resolution graphics package. The program uses new improved techniques in signal processing so that background effects may be minimized and an IR surveillance/detection system may improve its capabilities and optimize its performance.

The purpose of this thesis is to perform an evaluation of the BMAP code to provide future data to the IRSTD data processing and acquisition system which is now in its final stage of engineering development. For that reason the adaptation/use of the BMAP program was made by transferring data from the main program to a Masscomp computer associated with the IRSTD. The image data were located in three files called BEDFORD files, named after the place in which the experiment took place, Bedford Ma. The data was collected there from 10 to 14 September 1984. The observations were made at a hole between clouds in the sky backlighted by the sun using a dual scanning radiometer in the 4 to 5 micrometer and 8 to 11 micrometer bands. The detectors consisted of 16 element arrays. For the experiment it was assumed that the

clouds were constituted of water droplets with a logarithmic size distribution and a mean radius of 4 micrometers.

The present work consists of ten chapters and four appendices after the present introduction. In the first and second chapter a theoretical overview of the background problem is presented. In the third chapter the problems, related to target tracking, of the various background radiances are discussed including references to the marine background. The fourth and fifth chapter are about the main NSWC clutter code (in conjunction with the BMAP source code), presenting an adaptation of the program with its full capabilities including the LOWTRANS code, and highlighting some important aspects for the future user. In the sixth chapter a discussion of the collected data with the BMAP is presented including the method to enter that data into the Masscomp part of the IRSTD using different computer algorithms. The sixth chapter presents the format in which the image data are arranged inside the Bedford files so that they can easily be transferred from one system to the other; also a method for extraction of the image data from the BEDFORD files is discussed. In the seventh chapter we have a presentation of the organization of data inside the Masscomp computer of the IRSTD including the method of transfer of the data, already extracted from the BEDFORD files, to magnetic tape in the Masscomp computer. In the eighth chapter a connection between the data format of the portable AGA

Infrared System and the formats of the NSWC clutter code and MASSCOMP is made. In the ninth chapter an analysis of the method of extracting the data from the BEDFORD files is made. Finally in the last chapter conclusions and recommendations for future work are made.

In Appendix A the LOWIN and LOWPLOT cards of the mainframe program LOWTRAN6 found as an option inside the BMAP program are presented; in Appendix B the computer algorithm to extract the image data from the BEDFORD files is listed.

Appendix C provides a useful description in a few words, for the future user, of the "F1...F10" keys of the IBM computer in use with the NSWC clutter code program. Finally Appendix D contains the computer software initially provided by the ONTAR company to read the BEDFORD files.

It is expected that the results from this work will provide a start to further development of the BMAP program for use with the IRSTD system (always considering the limited capabilities of a small portable computer) by transferring data from other infrared detection systems, such as the AGA Thermovision 780, into the BMAP and later using the computer routines of this thesis to transfer the infrared image data to the IRSTD. Furthermore it is expected that this work will give a good understanding of the background problems which may appear in an environmental infrared scene.

## II. THE BACKGROUND PROBLEM

### A. BACKGROUNDS AND TARGETS

An infrared system must receive the radiation from the target, identify it as an input signal, and distinguish it against all background radiation within the field of view. But since all objects which have a temperature above absolute zero radiate energy in the infrared, that background radiation is omnipresent, causing noise in the optical system. This is called the external noise and has two different components [Ref.3]. The first component is called the spatial component, caused by the different structural details of the environment and the second component is called the temporal component, which is actually a photon noise, caused by the fluctuations of the photons emitted from the background (proportional to the square root of the number of the photons). These photons cause a modulated flux on the detector called "Background-Radiation Photon Noise". The lower limit for the detector's noise, and hence the best detectivity, is determined by these fluctuations. Using the Planck's law and the Bose-Einstein statistics, knowing the environmental conditions, we can calculate the background photon noise.

### B. SPATIAL BACKGROUND RADIANCE (NOISE)

The spatial background noise can be produced by many factors such as sunlight scattered from atmospheric particles

like water droplets, fog, haze and clouds, or from sunlight reflected from the sea surface/terrain or self emission of different objects like the sun, stars and planets or objects on the surface of the earth like people, trees, etc. There are two different kinds of spectral background radiance:

1. Celestial background
2. Terrestrial background

The celestial background is the radiance due to the sun, moon, and planets which affect space-based optical systems looking out to space. This is important for many applications but not for the subject of this thesis.

The terrestrial background is the radiance coming from various sources inside the earth's atmosphere. This background can be considered to arise mainly from three sources:

1. the scattering of solar radiation by the earth or clouds or the sea,
2. the emission from different molecules in the atmosphere such as carbon dioxide, ozone molecules and water vapor, and
3. the emission of surface objects like trees, power plants, sand, people, houses, etc.

The full analysis of various terrestrial backgrounds is given on Chapter III of this thesis.

### C. TARGET-BACKGROUND BRIGHTNESS/TEMPERATURE DIFFERENCE

One of the most important factors in the detection probability of a target is the radiance difference between a target and its surrounding background. That radiance can be expressed with the radiation contrast described in Ref.3 with respect to the brightness as:

$$C = \frac{B_o - B_b}{B_b} \quad \text{when } B_o > B_b \quad (2-1)$$

or

$$C = \frac{B_b - B_o}{B_b} = \frac{\delta B}{B_b} \quad \text{when } B_o < B_b \quad (2-2)$$

where  $C$  = radiation contrast

$B_b$  = average brightness of the background where the target is located,

$B_o$  = target's brightness, and

$\delta B$  = incremental brightness of the target from the average background  $B_b$ .

The contrast  $C$  may vary from 0% to 100% if the target is darker than the background. If, on the other hand, the target is brighter than the background then the  $C$  may vary from 0 to infinity.

The detection of a target against the background depends on the background brightness and the size of the target. Figure 2.1 [Ref.3] presents the threshold contrast vs. background brightness for various angular sizes (in minutes) of the target.



Another method of describing the contrast factor [Ref.1], named the "Radiation Contrast Factor" CR, is in terms of the apparent temperature difference between the target and its background environment. CR is defined from the equation:

$$CR = \frac{W_T - W_B}{W_T + W_B} \quad (2-3)$$

where  $W_B$  = Background radiant emittance ( $W/m^2$ ) and

$W_T$  = Target emittance ( $W/m^2$ ).

Since  $W_T = \epsilon \sigma T^4$  then:

$$CR = 2\delta T / T_b \quad \text{for } \delta T \ll T \quad (2-4)$$

where  $\delta T = W_T - W_B$

$T_T$  = Target temperature

$T_b$  = Background temperature

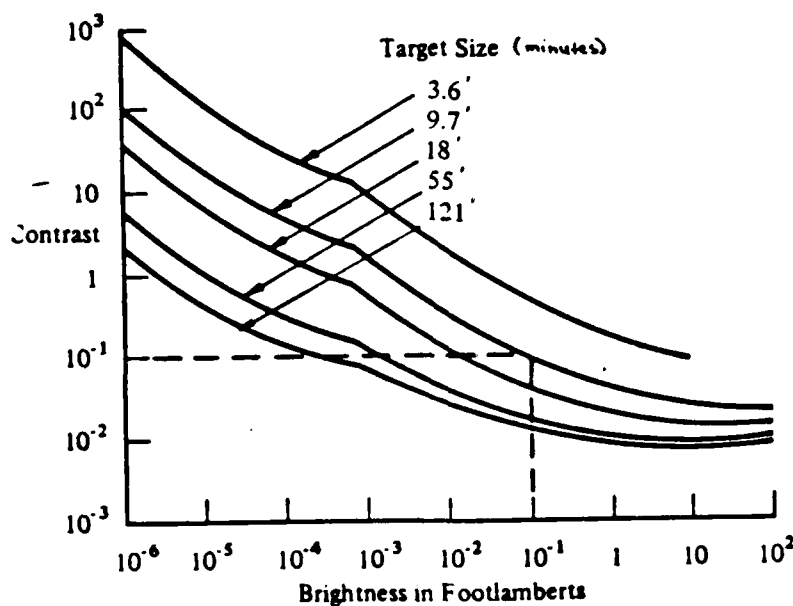


Figure 2.1 Threshold Contrast versus Background Brightness  
(From Ref.3)

In the case of small temperature differences between the background and the target, the radiation contrast factor becomes very small and the detection of the target becomes very difficult.

The radiation contrast as a function of the target-to-background temperature difference is shown in Figures 2.2 and 2.3 describing the radiation contrast for the 3 to 5 and the 8 to 14 micrometers infrared band. In these figures the vertical axis represents the Radiation Contrast factor and the horizontal axis represents the temperature difference between the target and the background for various background temperature values (from 240 K to 300 K).

A good example of radiation contrast is presented by Seyrafi in Ref.3 describing an experiment involving a truck, parked in an open field and observed over a 24 hour period with an infrared optical system. In the experiment it was observed that the contrast between the vehicle and the background varied from positive values in the daytime to negative values during the night passing through zero (equal temperature) twice a day. More specifically the truck in the afternoon gave a positive contrast value which increased up to a maximum value. At night, after passing from the equal temperature value, the truck was cooled faster than background so that the contrast value became positive again and the cycle continued. As the difference in temperature

between the target and the background increases the potential between the target and the background increases the potential acquisition range increases too as presented in Figure 2.4 [Ref.4]. In the figure we show the acquisition range for a target as a function of target-to-background temperature difference. Also the increase in the temperature difference leads to an increase in the range for identification and classification of a potential target. In Figure 2.5 [Ref.4] we have a range prediction for identification and classification of a target with respect to target-background temperature difference in degrees Kelvin.

#### D. SPECTRAL-SPATIAL DISCRIMINATION (CLUTTER SUPPRESSION)

The process of encoding the target's information against the background suffers from the problem that the signals from the background will also be processed and modulated like a real target. A system is said to be background noise limited when the unwanted signals or noise from the environment exceed the other noise sources of the system. When we scan the different background objects, the noise created will depend on their spatial distribution, spectral radiance, and on the encoding and processing method employed.

In one target discrimination model [Ref.5] a distribution of background noise amplitude is obtained and a threshold noise level set on the basis of expected frequency of occurrence according to environmental conditions set.

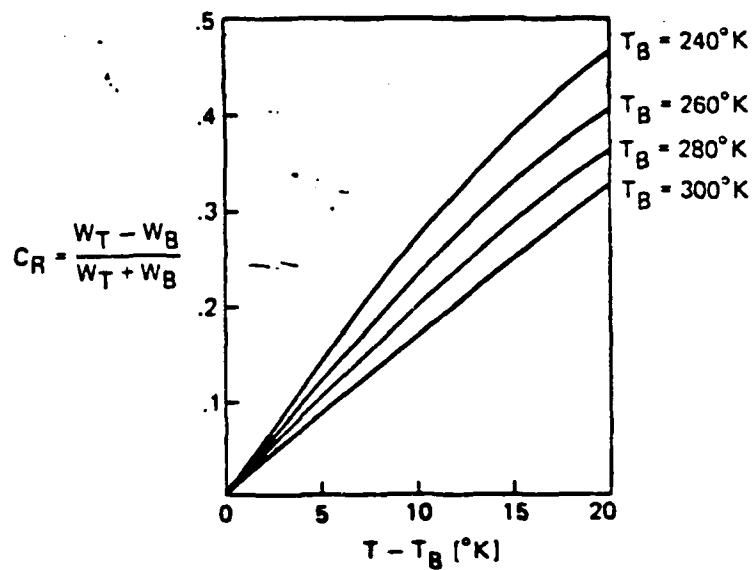


Figure 2.2 Radiation contrast for the 3.5 to 5  $\mu\text{m}$  band  
(From Ref.3)

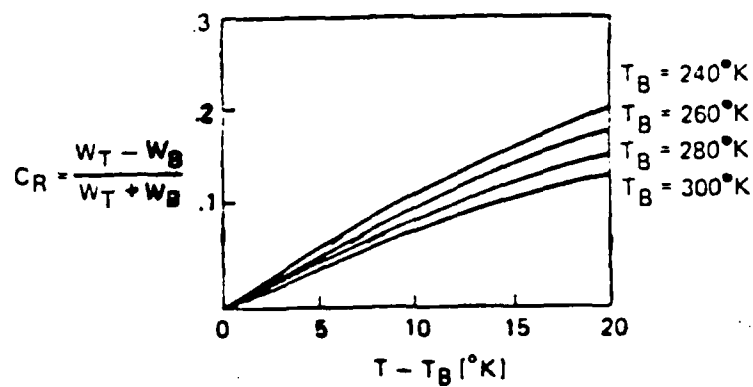


Figure 2.3 Radiation contrast for the 8 to 14  $\mu\text{m}$  band  
(From Ref.3)

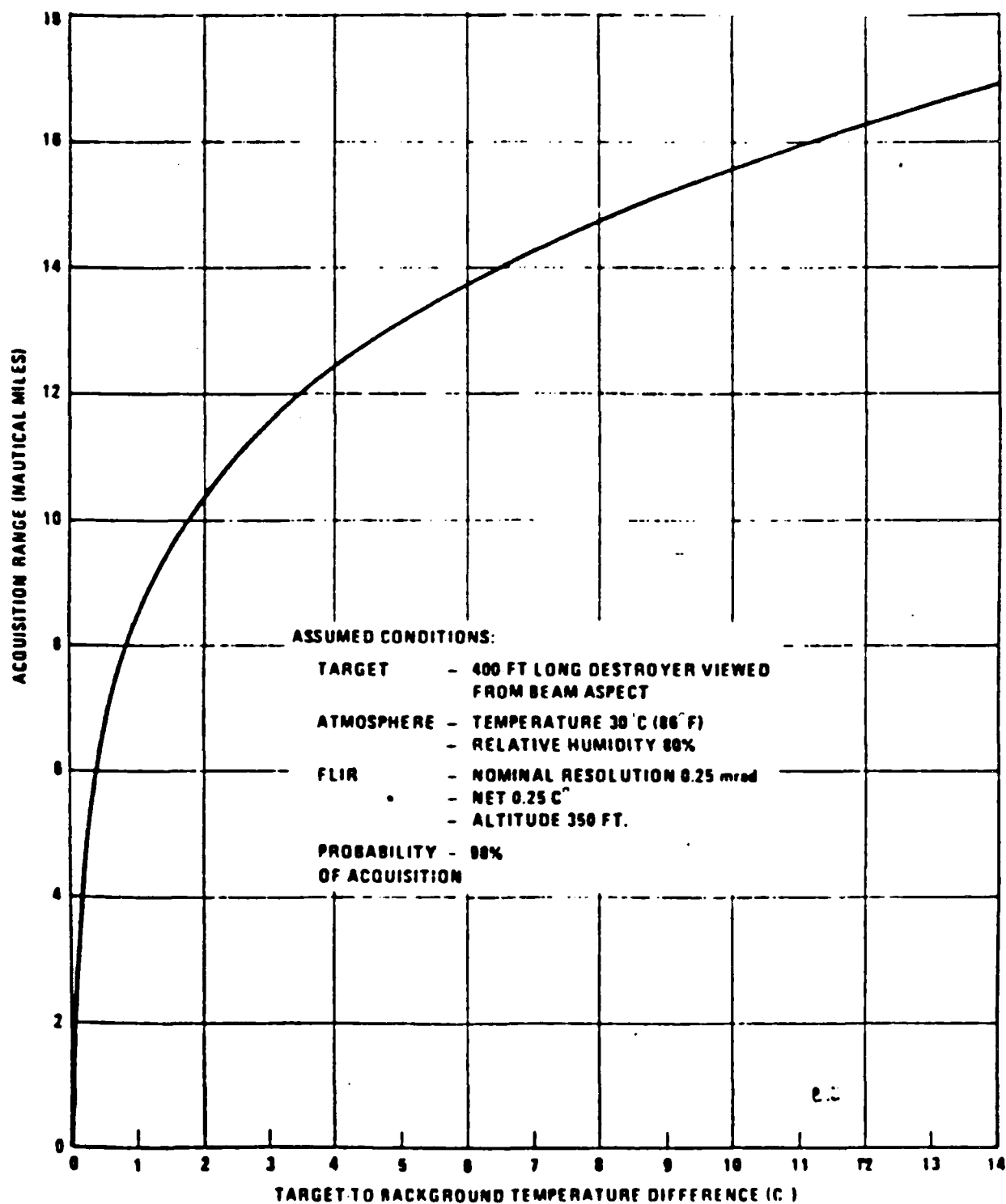


Figure 2.4 Target Acquisition Range as a Function of Target to Background Temperature Difference (From Ref.4)

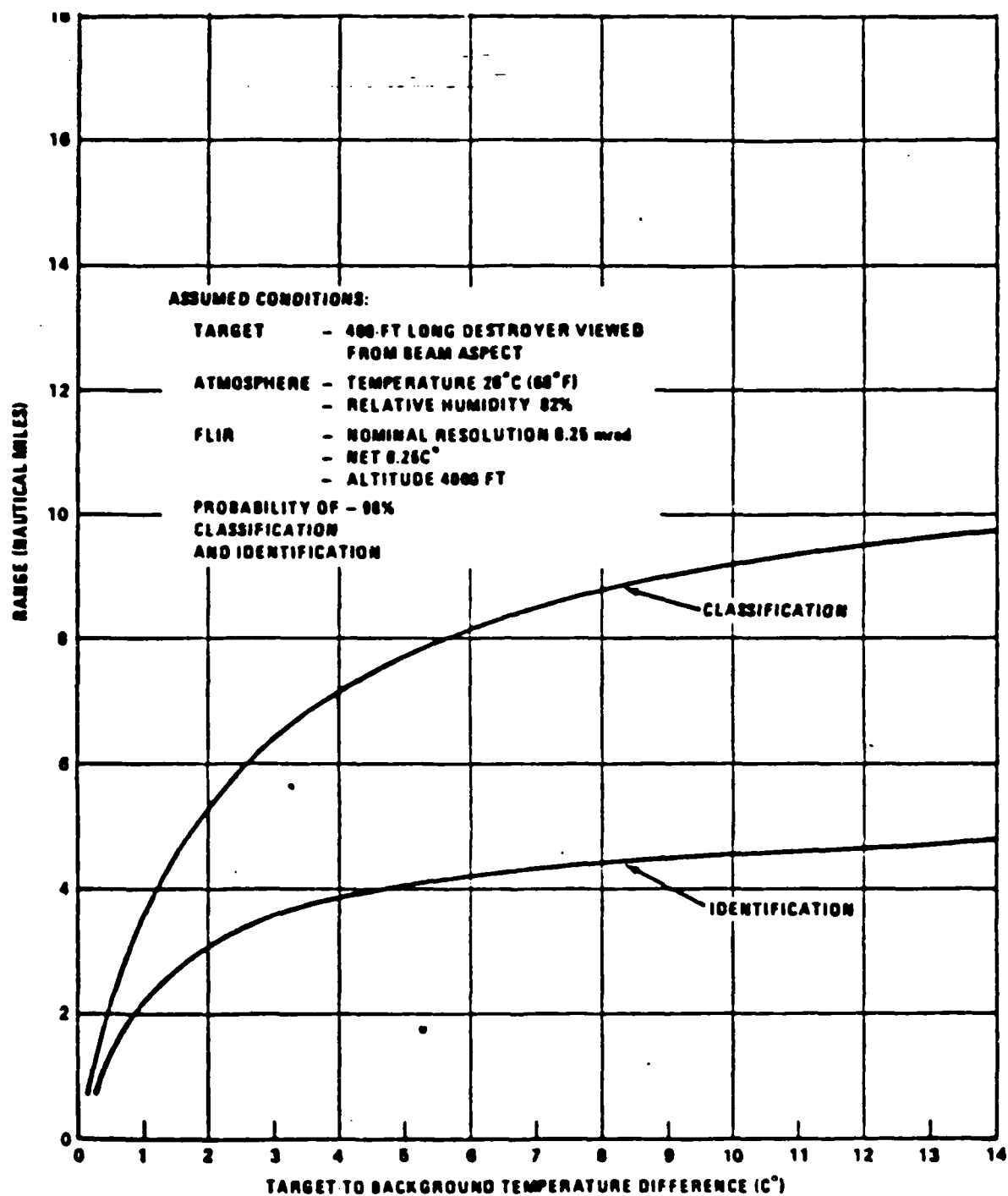


Figure 2.5 Target Classification and Indentification Ranges as a Function of Targey to Background Temperature Difference (From Ref.4)

Another model [Ref.5] uses the "Wiener Spectrum" which is a Fourier transform of a two-dimensional autocorrelation function. This is the most effective method of describing the spatial variations of background radiance with respect to confirming the mathematical model with the real physical conditions.

Finally we can say that the value of the limiting noise is largely dependent on the electronic filtering, the spatial filtering, the spectral filtering and all the other filtering that can be applied to the signal regardless of the mathematical model used to describe the background noise. That is the only way to achieve a background noise limited system.

In infrared devices we have a spectral discrimination which is due to the spectral response of the detector/filter. To achieve maximum average contrast we use different statistical methods depending on the application. If we attempt to detect a target signal  $S(\lambda) = [\tau(\lambda) - b(\lambda)]$  where  $\tau(\lambda)$  is the target emitted power in the presence of a background random signal  $b(\lambda)$  and taking in account the preamplifiers noise  $N$  (independent of the choice of the filter) then to increase the average contrast between the target signal and the average background signal we must have a filter whose function  $f(\lambda)$  must maximize the ratio in equation (2-5):

$$\frac{\int_0^{\infty} f(\lambda) S(\lambda) d\lambda}{\int_0^{\infty} f(\lambda) b(\lambda) d\lambda + N} \quad (2-5)$$

Where  $S(\lambda)$  is the average radiant power as a function of the wavelength,  $b(\lambda)$  is the average variation in background radiant power as a function of wavelength. (A complete presentation of this filter analysis is presented by Khalil Seyrafi in Ref.3).

#### E. WIENER SPECTRUM/POWER SPECTRAL DENSITY

The power spectral density function, often called the Wiener spectrum, is a representation of the statistical characteristics in the frequency domain of the random input autocorrelation function. In a time-invariant system, for linear response in a stationary random process, we usually use the power spectral density function to derive the mean square response for the input variable and the appropriate transfer function.

In the specific case of a tracking loop analysis the most practical method for time response is to represent the inputs by random time series input signals and to use Monte Carlo statistical methods, as will be presented later, to find the power spectral density function.

We will specify the average domain with "w" [Ref.5] and we identify a sample  $S_w(y)$  in a random scene radiation



distribution  $S_w(x)$  for a two dimensional process. The average  $\Phi(x)$  (an autocorrelation with  $y$  a displacement variable in the same direction as  $x$ ) can be written as:

$$\Phi(x) = \int_{-\infty}^{+\infty} S_w(y) S_w(x+y) dy \quad (2-6)$$

The fourier transform of  $\Phi(x)$  is called the Wiener Spectrum of the scene and is defined with  $W(k)$  as:

$$W(k) = \int_{-\infty}^{+\infty} \Phi(x) e^{-\pi i k \cdot x} dx \quad (2-7)$$

The Wiener spectrum actually gives a full description of the statistical properties of a gaussian process and it is a function of two variables but can be specified completely as a function of a single spatial frequency variable.

The autocorrelation function and the Wiener spectrum are a fourier transform pair because both contain the same basic information about a random process, but in practice the Wiener spectrum is a easier representation since the convolution of the space functions is replaced by a product of functions of spatial frequency. So if we want to analyze a system's performance it is better to use the Wiener spectrum in order to manipulate aperture and image functions than to use convolution equations.

The Wiener spectrum can be measured in many ways. Figure 2.6 [Ref.7] provides a representation of various methods of

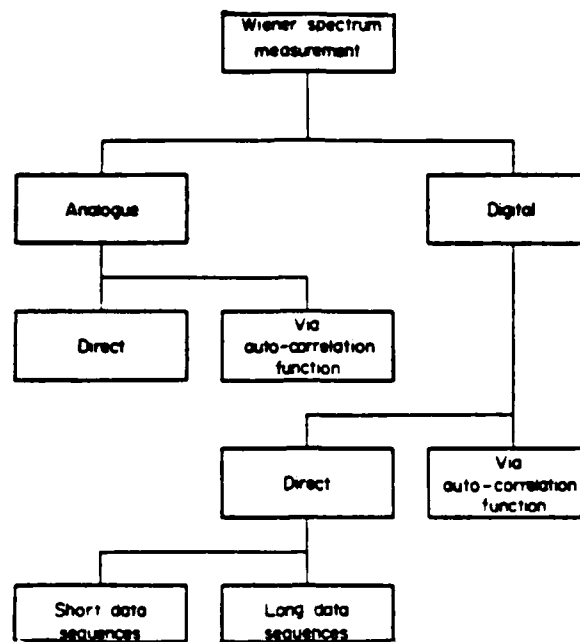


Figure 2.6 Techniques for measuring Wiener spectra  
(From Ref.7)

measuring this spectrum which can be implemented either by digital or analog techniques.

To get a significant target signal its surrounding background we must maximize the ratio of the instantaneous target signal squared divided by the mean squared background signal which is the following expression [Ref.8]:

$$\frac{\left| -\infty \int^{+\infty} A^*(k) T(k) dk \right|^2}{-\infty \int^{+\infty} |A(k)|^2 W_B(k) dk} \quad (2-8)$$

where  $T(k)$  = Fourier transform of target's distribution,

$A(k)$  = Fourier transform of the detecting aperture, and

$W_B(k)$  = Wiener spectrum of the background.

By using the background Wiener spectrum and the target radiance function we can create various space filtering cases in which the spectrum must be selected according to the environment of the target and similar statistical characteristics. We are actually concerned with the peak-signal to rms background-noise ratio at the output of the system radiation detector. For that reason we must choose a mathematical description of a space filtering field that will give us the wanted maximum.

The Wiener spectrum has some limitations too. The first one is the assumption that the spectrum has a quadratic probability density. Under that assumption we come up against the problem that a quadratic function for some negative values of the argument must take real values. But we can't give negative values to the spectrum of the radiance because it is always positive valued. The best we can do in solving the problem is to consider zero values in the place of the negative values of the argument for the random radiance process.

The second limitation is that when we examine the instantaneous field of view (IFOV) of a system for a cloudy environment we cannot apply the central limit theorem [Ref.8] because the detector can capture only a few shots of the cloud form and the characteristics of the infrared background fluctuations. As a result we cannot determine the higher moments of the joint probability functions. We can however

make better predictions of peaks of the background noise by measurements of the statistics of phase relationships and higher moments.

We can take for example a partially clouded sky and prove that a background scene must be described by more than one principal peak in the power density spectra. The scene considered could for example have a bimodal distribution with two peaks in which one at the lower radiance values describes the space between the clouds and the other describes the scattering and reflection in clouds with a range of radiance level of high probability. In that situation we could have problems describing the probability density function with a gaussian curve because it would not represent the actual scene. These problems are most obvious in the case of calculations of false probabilities in which the Wiener spectra are not appropriate background descriptions.

#### F. MONTE CARLO SCATTERING

The Monte Carlo procedure is a statistical method to describe a complicated set of physical processes of photon transmittance in the atmosphere.

When the observer and the emitting source directions are determined we need a large number of trial photons because until the calculation is finished we do not have any information about the exit direction of each photon. We can improve this by accumulating the exiting photons in angular

bins. We can track each photon until it makes a predetermined number of scattering events or leaves the cloud. The ratio of the scattering to the total cross section (IR single scatter albedo) is smaller than 1.0 (the ratio usually varies from 0.5 to 0.9) so that after a finite number of scattering events (about 20 to 50), the photon becomes insignificant and can be dropped.

To describe Monte Carlo scattering we must select random values in the range (a,b) which are then normalized in order to be inside the range 0 to 1. That can be done by using the equation:

$$B = \frac{\int_{-\infty}^{+\infty} i(a,x) F(x) dx}{\int_{-\infty}^{+\infty} i(a,b) F(x) dx} \quad (2-9)$$

where  $F(x)$  = Function defining the values of the parameter,  
and  $B$  = randomly selected value.

We then invert the equation to give the corresponding value of  $x$ .

The whole process must be made in a reasonable amount of time to obtain meaningful results and is described in the following way:

1. We first calculate the spectral weighing function from the atmospheric transmittance, solar irradiance and instrument response. By random selection in the interval we calculate the wavelength of each photon

and then from the tabulated values we determine its albedo and its scattering phase function.

2. The photon propagating through the cloud for a distance  $R$ , determined by a Monte Carlo selection, encounters an aerosol. We then make a check to investigate whether the potential scattering event is inside the cloud. We continue the calculations from step 4 if we find that the photon has escaped from the cloud, either from the sides, top, or bottom..
3. From the two Monte Carlo selections for the scattering angle we determine a new direction for the scattered photon. In the first Monte Carlo selection we pick the azimuthal angle with the assumption that all values are equally probable. In the second Monte Carlo selection we pick the scattering angle using the Henyey-Greenstein function (Ref 5). We then repeat step 2 with the new direction from the scattering point.
4. When the photon exits the cloud it is binned according to its escape angle. We then tabulate the reflected and transmitted escapes and obtain the total scattering probability by assigning a weighting function  $W^n$  in which  $W$  is the single scattering albedo and the  $n$  is the total number of scattering.
5. The procedure is then repeated for a new photon and, when we have completed the process for the assigned

number of photons, we calculate the distribution functions.

6. We can predict the amount of the incident energy coming out in a certain direction by the number of the photons in the same angular bin. We then select the bin and get the scattered intensity for the specified observer direction and as a by product we also get the distributions for all the other directions too. We can also improve the statistical uncertainty, when it is too big, by averaging the distributions over several angular bins.

The method by which the Monte Carlo method is implemented in the BMAP program is presented in Chapter V of this thesis.

### III. RADIANCE IN THE BACKGROUND PROBLEM

#### A. SPECTRAL RADIANCE OF THE SKY

##### 1. Introduction

For a good analytical presentation and understanding of the background radiation problem it is important to have a good knowledge of the sources that cause it. Sky radiance is caused mainly by two sources:

- a) scattering of solar radiation, and
- b) emission of the various atmospheric molecules such as CO<sub>2</sub>, ozone and water vapor.

##### 2. Scattering

The scattering of radiation in the atmosphere occurs by extracting energy from the incident light and, taking the center of the particle as origin, reradiating that energy into a  $4\pi$  solid angle.

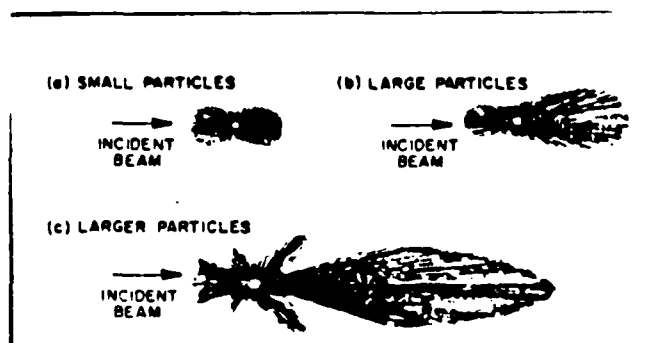


Figure 3.1 Scattering patterns (From Ref.6)



This scattering depends on the particle's isotropy, refractive index and its size relative to the wavelength. In Figure 3.1 [Ref.6] we have three scattering patterns from three different sizes of particle.

- a) When the particle is smaller than  $1/10$  of the radiation wavelength, we have symmetric scattering in the backward and forward direction.
- b) When the particle is of size  $1/4$  of the lights wavelength we have larger scattering in the forward direction.
- c) When the particle is of larger size than the wavelength we start observing side lobes.

The wave which is scattered is polarized by a small amount but since the wavelength remains unchanged we have no loss of energy. The scattering phenomena can vary according to the size of the particles found in the atmosphere which are:

<u>TYPE</u>	<u>RADIUS (<math>\mu\text{m}</math>)</u>	<u>CONCENTRATION (<math>\text{No}/\text{cm}^3</math>)</u>
Air molecule	$10^{-4}$	$10^{19}$
Aitkem nucleus	$10^{-3}-10^{-2}$	$10^4-10^2$
Haze particles	$10^{-2}-1$	$10^3-10$
Fog droplet	$1-10$	$100-10$
Cloud droplet	$1-10$	$300-10$
Raindrops	$10^2-10^4$	$10^{-2}-10^{-3}$

The case of molecular scattering is most commonly known as the "Rayleigh scattering" and varies proportionally to the

second power of the particle volume and is inversely proportional to the fourth power of the wavelength [Ref.10].

The other case of scattering is that caused by larger particles (usually of irregular shape) and is usually known as "Mie scattering"; here the common assumption is that all atmospheric particles regardless of size may be considered as isotropic spheres. In the limit of small sizes Mie scattering includes Rayleigh scattering.

### 3. Emission of atmospheric particles

According to Kirchoff's law [Ref.6]  $\epsilon = I/I_b$  where  $\epsilon$  is the radiant emissivity of a particular surface,  $I$  is the total radiant power per unit area emitted from the surface and  $I_b$  is the total radiant power per unit area emitted from a blackbody of the same temperature. The atmospheric gases of various species produce emission of radiation according to their absorption bands. For the most common temperature found in the atmosphere almost all of the radiant energy is between 3 and 30  $\mu\text{m}$  with the maximum (blackbody) peak occurring at 10  $\mu\text{m}$  with a value of  $10^{-3}$  watt  $\text{cm}^{-2}$   $\mu\text{m}^{-1}$  steradian $^{-1}$ . The reason is that the effective temperature is usually at the range from 200 to 300 K, so that the blackbody radiance gives the most probable value for the emitted radiance.

The maximum radiance of the sun occurs at a wavelength of about 0.5  $\mu\text{m}$ , since it radiates like a 6000 K blackbody, with a value of  $3 \times 10^{-2}$  watt  $\mu^{-1}$  steradian $^{-1}$  [Ref.6].

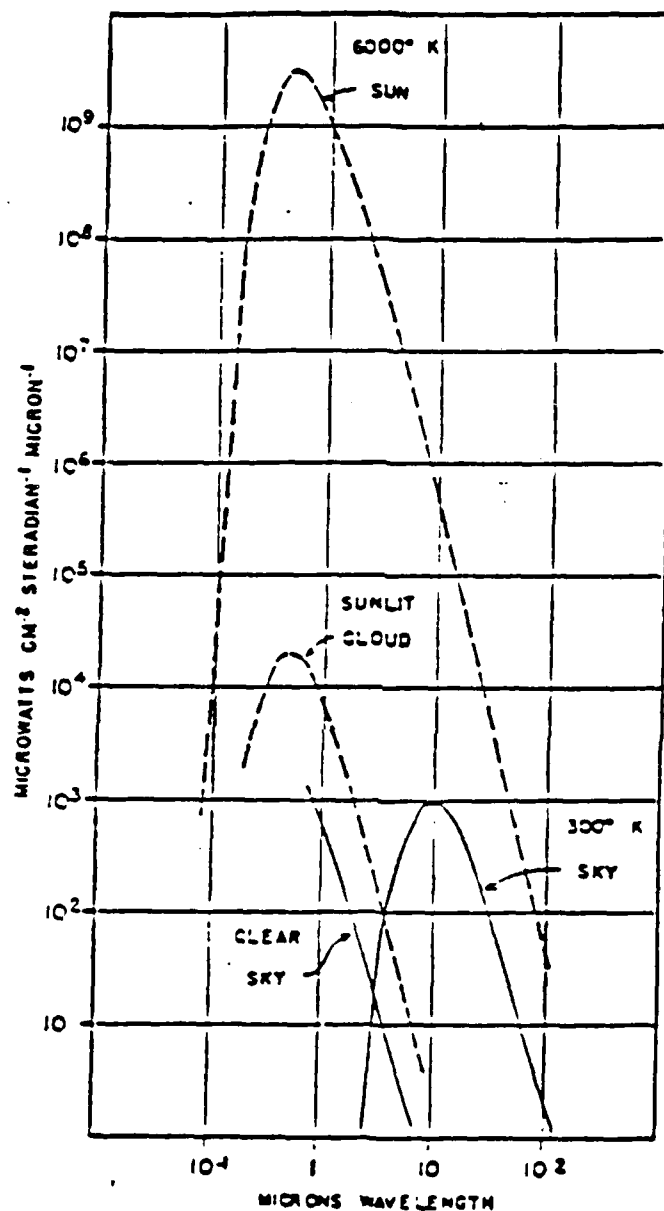


Figure 3.2 Spectral radiance of the sky in a idealized form  
(From Ref.9)

It has been found experimentally that the scattered sunlight radiance and the molecular emission radiance in the range 3 to 4  $\mu\text{m}$  are equal [Ref.6].

When we go to shorter wavelengths the molecular emission can be ignored in the daytime and has a very small value at night because the scattered sunlight has a much larger value. The situation changes when we go to wavelengths above 4  $\mu\text{m}$ . There the scattered sunlight can be ignored since the molecular emission is much greater. In Figure 3.2 [Ref.9] we have a presentation of the spectral radiance of the sky with the sun radiating, as mentioned before, as a 6000 K blackbody and the sky as a 300 K blackbody. From the figure we can see that we have a uniform diffusion of the radiance due to solar radiation presented by the "sunlit cloud curve".

The average radiance is approximately  $2 \times 10^{-5}$  times the sun's radiance, although practically only 1/10 of the maximum spectral radiance is scattered. In the figure this is presented as the "clear sky curve".

#### B. SPECTRAL RADIANCE ABOVE 3 $\mu\text{m}$ - CLEAR SKY

The spectral radiance is a product of a blackbody's radiance, varying with temperature, and of the emissivity depending on the number of the emitting molecules along a path. Hence the spectral radiance of the sky strongly depends on the following:

- 1) air temperature

- 2) water-vapor content of the atmosphere
- 3) ozone, and
- 4) elevation angle from the horizon.

The dependance of sky spectral radiance on elevation angle is presented in Figure 3.3 [Ref.6]. In that figure we have the spectral radiance of a clear night sky at 11000 feet above sea level and ambient temperature of 8° C for elevations of: 0°, 1.8°, 3.6°, 7.2°, 14.5°, 30° and 90°. From the figure we can see that we have only weak absorption lines in the 8 to 13  $\mu\text{m}$  region so we have some slight dips.

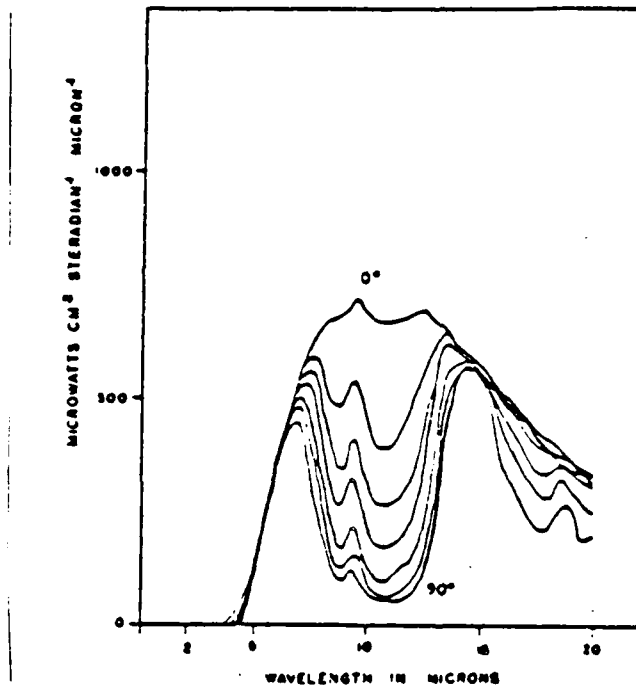


Figure 3.3 Spectral radiance of a clear night sky at Colorado  
(From Ref.6)

For the path at 0° elevation we have a finite air mass because of the earth's curvature and we have almost blackbody radiation ( $\epsilon=1$ ). If we increase the elevation angle we see

that the spectral radiance decreases and we no longer have blackbody emissivity. The emissivity for elevation angles near the zenith is low at the regions from 8 to 13  $\mu\text{m}$ , and the spectral emissivity is almost unity for the water vapor band of 6.3  $\mu\text{m}$  and the carbon dioxide band of 15  $\mu\text{m}$ . We can also see a peak emission at 9.6  $\mu\text{m}$  because of the ozone.

The spectral radiance is highly dependent on the ambient temperature. From Figure 3.4 [Ref.6] we can see the spectral radiance of a clear sky with an ambient temperature of 27° C and elevation angles of 0°, 1.8°, 3.6°, 7.2°, 14.5°, 30°, and 90°.

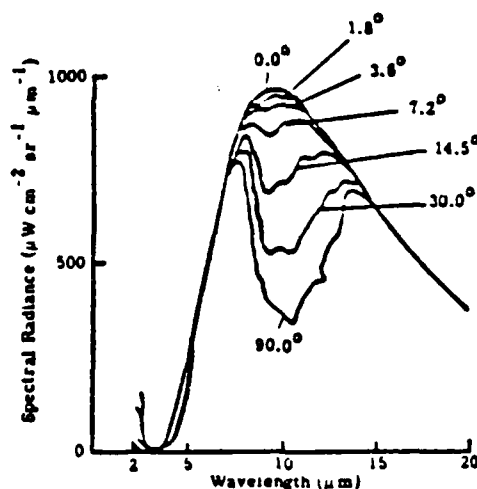


Figure 3.4 Spectral radiance of a clear sky at Florida  
(From Ref.6)

Comparing this figure with Figure 3.3 we can tell that the humid atmosphere of Florida at sea level makes the emissivity go to 1 for the wavelengths less than 7  $\mu\text{m}$  and higher than 15  $\mu\text{m}$ , because we have a greater air mass with larger quantities of water vapor and  $\text{CO}_2$ , but in the middle region of 8-13  $\mu\text{m}$  we have a higher emissivity for all elevation angles.

In Figure 3.5 we have a comparison of the spectral radiance for different ambient temperatures at Colorado (2.5° C and 27.5° C).

The dashed lines represent the black body spectral radiance for the ambient temperatures at the time of measurement.

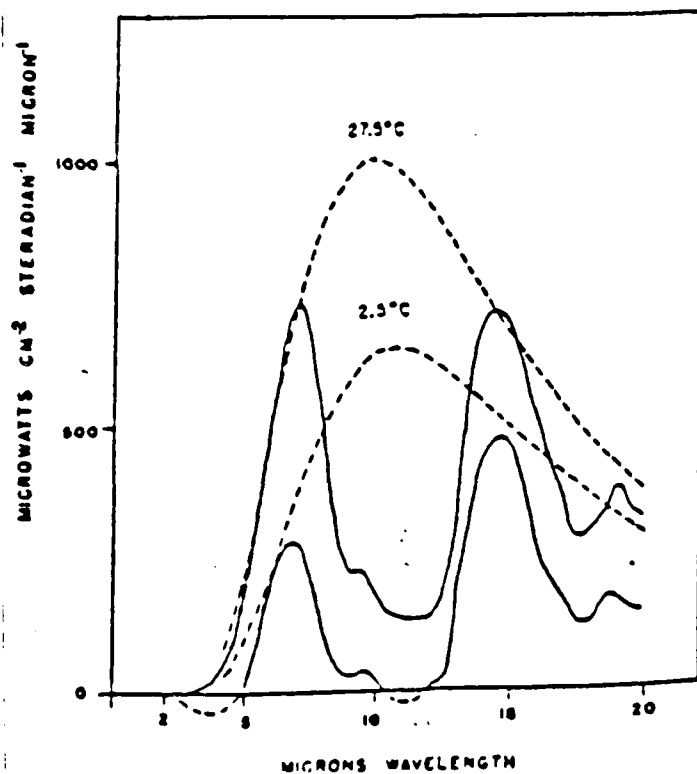


Figure 3.5 Comparison of spectral radiance for various temperatures in Colorado (From Ref.6)

We can see that we have spectral radiance almost at the blackbody limit for the wavelengths corresponding to the absorbing bands and completely different when we are out of this region because of the smaller emissivity and colder air mass since the atmospheric layer is at a greater distance from the observation point.

### C. CLOUD RADIANCE

The most common objects in the earth's atmosphere are clouds. The clouds can be separated according to altitude into three major types with subsequent variation as follows:

<u>LEVEL</u>	<u>HEIGHT OF EXISTENCE</u>	<u>TYPE OF CLOUDS</u>
Low	Earth's atmosphere to 2 Km	Stratus-Stratocumulus
Middle	2 - 7 Km	Alto cumulus Cirrostratus
High	5 - 13 Km	Cirrocumulus Cirrus

Their behavior is governed by the following rules:

- 1) they can scatter solar radiation,
- 2) they can emit radiation from their own body due to larger temperature from their surrounding environment, and
- 3) they can reflect radiation which originates from terrestrial objects.



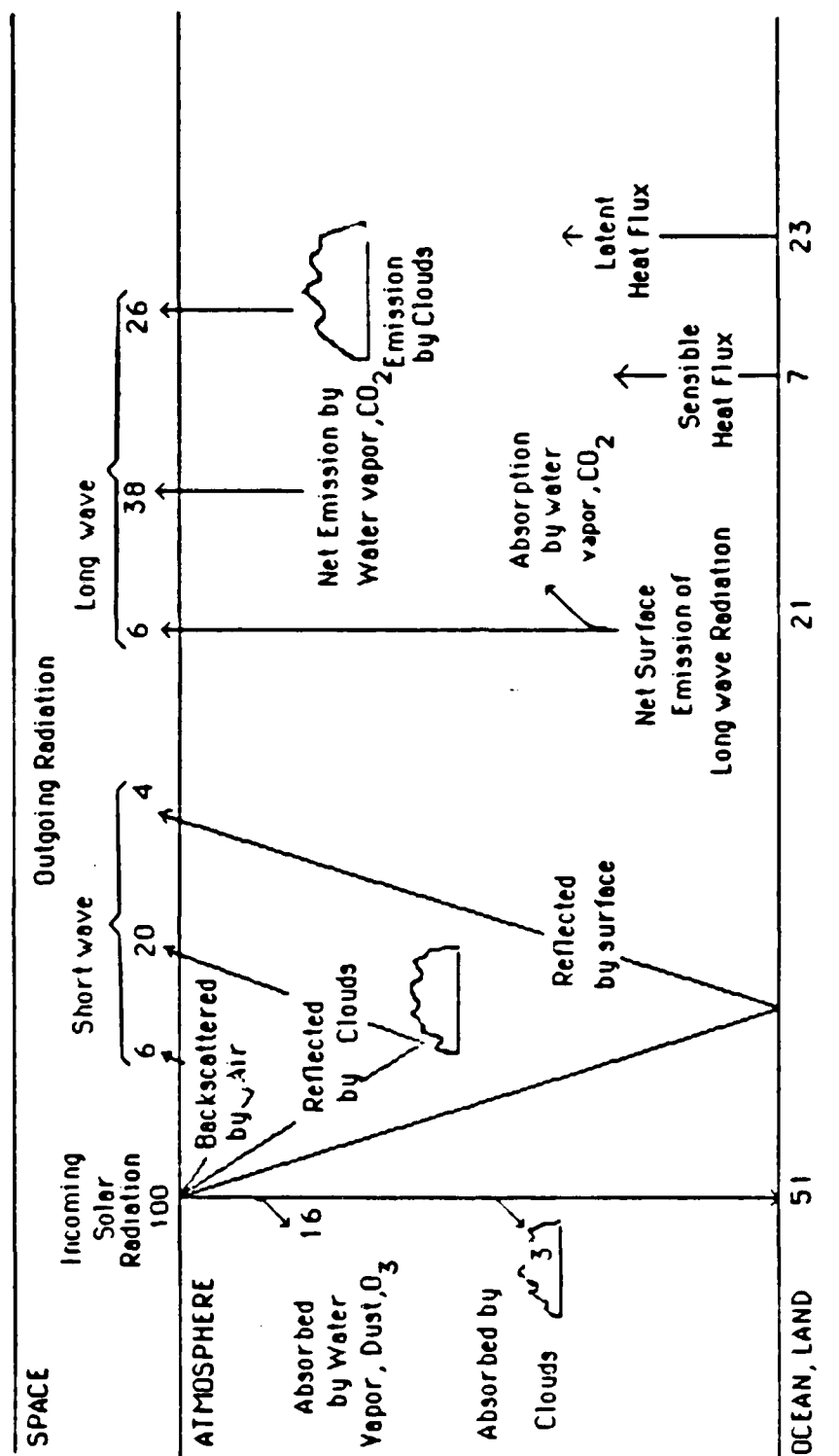


Figure 3.6 Thermal Radiation through clouds (From Ref.11)

The clouds contribute a major portion of the spectral radiation of the sky since by scattering the sunlight they become a source of radiation themselves. In order to do this they have some limitations of their own. They must not be less than 100  $\mu\text{m}$  in thickness and they must have droplet densities less than 0.5  $\text{g}/\text{cm}^2$ ; otherwise they behave like a blackbody with emissivity and absorption coefficient approaching unity.

Figure 3.6 [Ref.11] shows a schematic presentation of the reflection of thermal radiation by clouds. About 20% is reflected and 3% is absorbed while 26% of the radiation going back to space is originated by the clouds.

In Figure 3.7 [Ref.6] we have the spectral radiance of a dark cumulus cloud in which the dashed lines represent the cloud temperature ( $-10^\circ\text{C}$ ) and the ambient temperature of a blackbody.

When we come to higher elevations (cirrus clouds) the spectral radiance is represented by Figure 3.8 [Ref.6] for various elevation angles.

#### D. RADIATION OF AN OVERCAST SKY

The clouds in the atmosphere are composed of water droplets which absorb, refract and reflect the infrared radiation. In the visible region the clouds form a good diffuse reflector because the water droplets do not absorb any radiation. Figure 3.9 [Ref.11] shows the spectral

emissivity vs. wavelength for cloud layers of thickness  $\delta z$  measured in meters.

When we have an overcast sky, in which the highest cloud is at an elevation of 500 to 700 feet, then the radiance

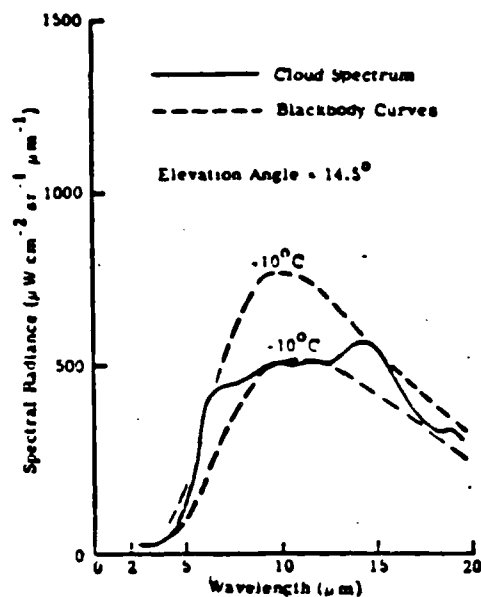


Figure 3.7 Spectral radiance of a dark cumulus cloud

(From Ref.11)

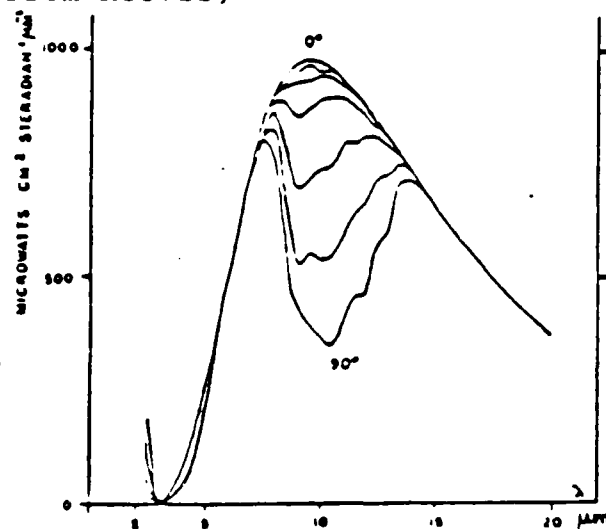


Figure 3.8 Spectral radiance for high altitudes (From Ref.6)

resembles that of a blackbody with the cloud's temperature except in the region of 5-8  $\mu\text{m}$ . In Figure 3.10 we have the integral emittance  $E$ , transmittance  $T$  and absorption  $A$  for cloud layers with thickness  $\delta z$  in meters.

On a cloudy day we have large variations of the average radiance because of the various ways the clouds can scatter the sunlight. For a water droplet the scattering is much greater in the forward direction than to the side. For that reason a thin cloud near the sun seems brighter than it would if it was further away.

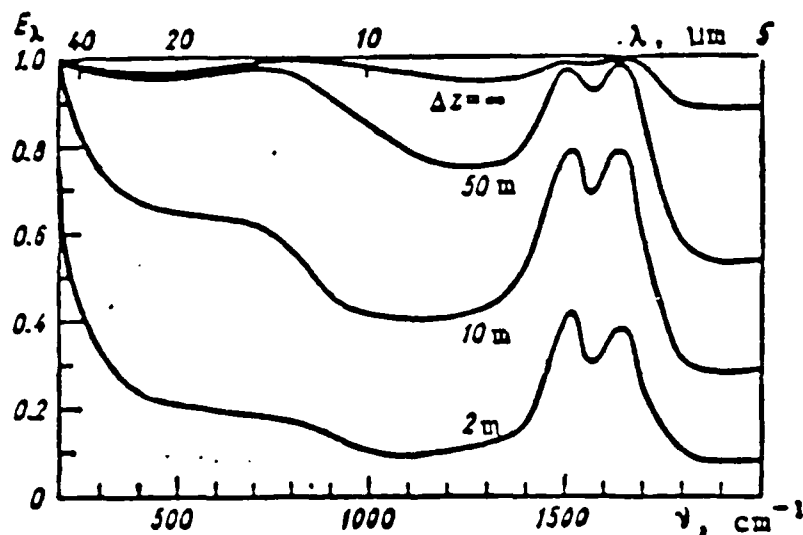


Figure 3.9 Spectral emissivity of cloud layers thickness  $\delta z$   
(From Ref. 11)

This phenomenon occurs mostly at the short wavelengths with a peak at about 3  $\mu\text{m}$ .

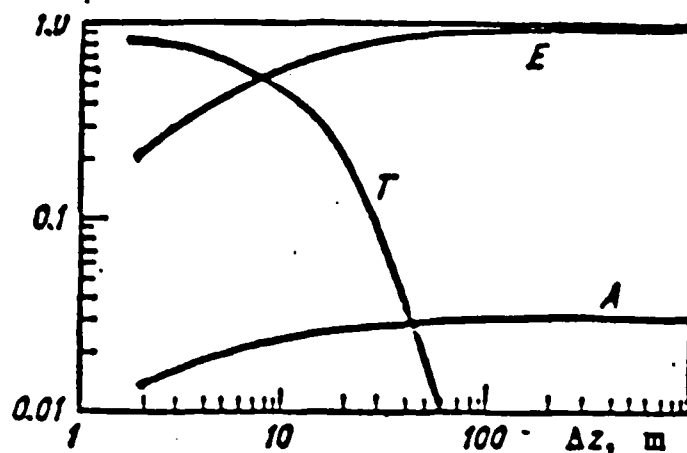


Figure 3.10 Spectral emissivity of cloud layer thickness  $\delta z$   
(From Ref.11)

## E. MARINE BACKGROUND RADIANCES

### 1. Introduction

The surface of the earth is covered by a great amount of water which has some unique optical properties since it is a poor emitter of radiation and a good reflector in the optical region of the spectrum. In the infrared region, though, water becomes a good emitter under certain circumstances. If the water were not disturbed by the waves, it would reflect the light like a mirror but, because of the wave pattern, which creates various surface elements, we have different orientations depending on the slope and height distribution of the waves.

In the IR region the reflection abilities of the sea water remain amplified by the good emission of the infrared radiation when the waves begin to break [Ref.6]. In the special case of foamy breaking waves we have a blackbody

behavior with a higher radiance for a rough sea than a calm one.

Generally the marine background radiance depends on the following parameters [Ref.5]:

- a. Material properties of the sea bottom,
- b. Temperature distribution of the sea's surface,
- c. Various optical properties of the sea water, and
- d. Wave slope distribution and surface geometry.

## 2. Material properties of the bottom

After penetrating into sea water, the solar radiation can scatter from the various particles in the sea water and from the bottom materials. This scattering occurs only in the 0.35 to 3.0  $\mu\text{m}$  region falling to the 0.4 to 0.7  $\mu\text{m}$  region for pure water. This scattering is not important for the analysis of this thesis.

## 3. Temperature distribution of the surface

The temperature distribution of the sea surface, ranging from 29° C at the equator to 0° C in the arctic regions, plays a major role in determining the total radiance of the sea. That radiance can be further effected by the presence of currents such as the Gulf Stream, giving variations of several degrees Celsius, but mostly is determined by the temperature variation from point to point.

From Figure 3.11 [Ref.12] we see a variation in temperature of 0.6° C in measurements made under evaporative conditions at the surface relative to measurements made one 1

mm below the surface. That slight cooler variation of the  $0.6^{\circ}\text{C}$  is due to radiation exchange rate of evaporation of the heat flow below and above the surface [Ref.5].

#### 4. Optical properties of sea water

The top layer, 0.01 cm of thickness, of sea water most determines the thermal radiance [Ref.5]. The subsurface part of the water does not create any radiation. At wavelengths above  $3\text{ }\mu\text{m}$  sea water is opaque. At wavelengths from 2 to  $4\text{ }\mu\text{m}$  the thermal emission of the surface is less than the reflected radiation which dominates the wavelength range covering 99.02% of the sun's total radiant energy.

That leaves only 0.08% for the 8 to  $14\text{ }\mu\text{m}$  region which is mostly effected by the thermal radiation. In Figures 3.12 through 3.14 [Ref.5] we have the emissivity and reflectance vs angle of incidence calculated from average data from 2 to  $15\text{ }\mu\text{m}$ , the reflection from sea water vs. wavelength and the incidences of refraction vs. wavelength of the sea water.

#### 5. Wave slope distribution and surface geometry

The surface geometry and wave slope distribution as presented by Cox, and Munk in Ref.12 play a major role in the refraction and reflection of the incident radiation on the sea surface.

In Figure 3.15 [Ref.5] we have the reflection of the solar radiation from a flat surface with  $\sigma=0$  and from a rough surface, caused by a wind of 4 Beaufort (11 to 16 knots), with  $\sigma=0.2$  (where  $\sigma$  represents the square root of the

variance of the wave slope distribution). From the figure we can observe that the albedo  $R$  on the vertical scale varies starting from a value of 0.02 when the sun is at the zenith ( $\phi=0^\circ$ ) up to 1 when the sun falls at the horizon ( $\phi=90^\circ$ ) for a flat sea. For the rough surface multiple reflections and shadowing begin to be effective causing the reflectance to fall to 20% near the horizon and the emissivity to rise to a value of 80%.

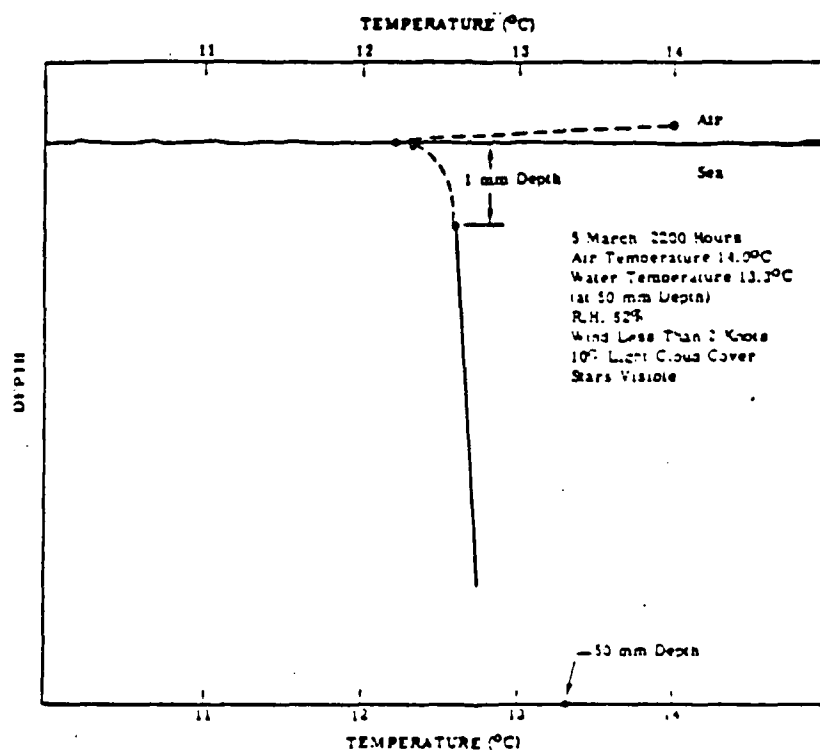


Figure 3.11 Thermal structure of the sea boundary layer  
 (From Ref. 5)





Figure 3.12 Reflection of sea water surface at 0°, 60° and 80° angle of incidence (From Ref.5)

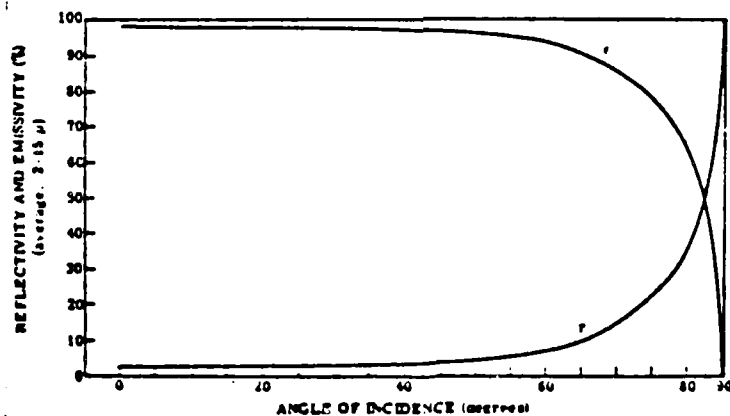


Figure 3.13 Reflectance and emissivity of water vs incidence (From Ref.5)

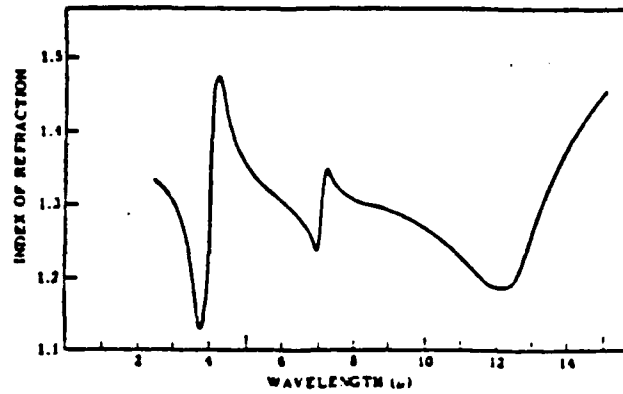


Figure 3.14 Index of refraction of sea water calculated from refractivity data (From Ref.5)

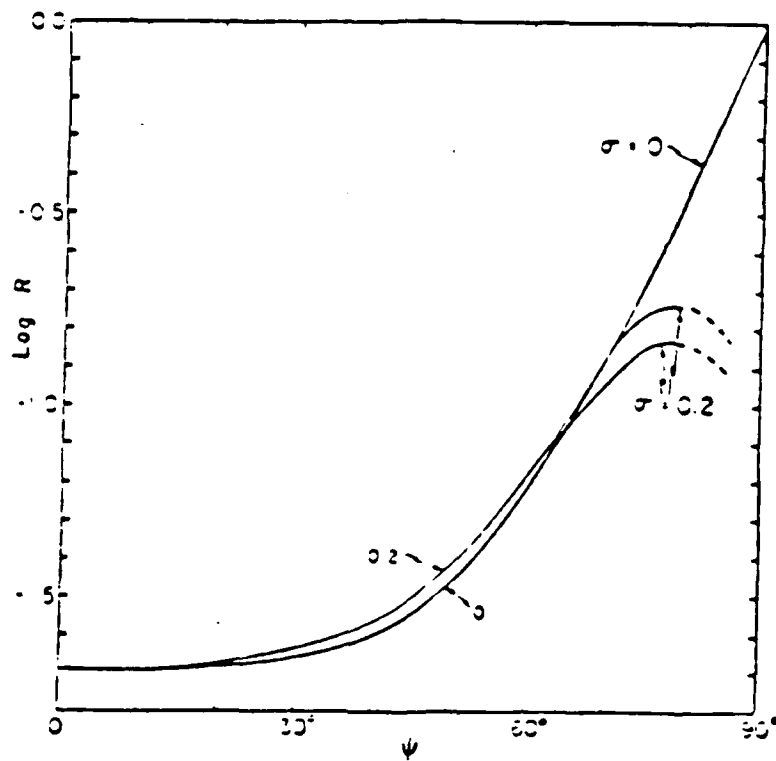


Figure 3.15 Reflection of solar radiation from a flat and from a rough sea surface (From Ref.5)

#### IV. THE BACKGROUND MEASUREMENTS AND ANALYSIS PROGRAM

##### A. GENERAL

###### 1. Introduction

The BMAP code is a program being developed by the ONTAR corporation as a supplement to the NSWC clutter code for use with the Navy's fleet defense systems under the requirement for detecting the infrared signature of a target against a clutter background. To achieve this requirement high spatial resolution data will be needed from various infrared sensors on airborne or surface based platforms over a wide area which will provide the required threat warning, acquisition and target tracking. The total field of view (TFOV) is to be searched continuously and, in combination with the small pixel size instantaneous field of view, results in a large throughput for the signal processors is needed. This will cause false alarms originating from the sea clutter and clouds that will put some limitations on the performance of the system.

For this reason in support of these defense systems the background measurements and analysis program was developed in support of the NSWC clutter code with the following capabilities [Ref.13 and 14]:

- a. Analysis and modeling of various background scenes.
- b. Acquisition of high quality background data
- c. Characterization of the IR scene's background clutter

The program model in including the NSWC clutter code is used in the following areas [Ref.14]:

- a. Collecting data: The program is to operate under field site conditions in a small IBM portable computer using real time data for the appropriate real time scenes and displaying that data on the screen as an infrared scene.
- b. Data analysis: The option of data analysis, and characterization of the data and other cloud scenes is available with respect to the atmospheric conditions and infrared real time scenarios.
- c. Modeling: The modeling option of the data and the sea clutter is also available, within signal processing, for calculating the radiance using Monte Carlo methods, irradiance and transmittance using LOWTRAN6 modeling .

## 2. Model Parameters (Present Version of BMAP)

For the current edition of the BMAP [Ref.16] the following assumptions have been made:

- a. Response of the instrument: In the present version of the BMAP the bandpass response for the BMAP instrument function in modeling is determined by the user. Future modified version of the code will determine the instrument response according to the wavelength.

- b. Geometry of the Clouds: The current edition of the BMAP assumes that the clouds under consideration are semi-infinite and variable cloud thickness can be determined using the Monte Carlo statistical method.
- c. Wavelength Bandwidth of Operation: The present source code is limited to the wavelength bandwidth region of 3 to 5 micrometers. The future edition of the BMAP will extend that region to the 8 to 12 micrometers wavelength band.
- d. Scattering Model: This model calculates the angular distribution of the clouds by using the phase function presented by Henyey and Greenstein [Ref.20] and various other parameters such as the Spectral Albedo and the Scattering Asymmetry. Zachor and Shette [Ref.21] determine some of these parameters for an average rain radius of 4 micrometers for the water droplet distribution used in the present version of the BMAP. This study [Ref.21] can be used for various droplet distributions, ranging from 2 to 32 micrometers. Some of these results will be implemented in the future modified edition of the BMAP.
- e. Geometrical Aspects of View: This determines whether the cloud is side lit and the scattered radiation creates the illuminated surface, or whether the cloud is backlit and the radiation from the sun, which is

behind the cloud, is passing through the mass of the cloud. The present version of the BMAP program assumes that the observation is being made from the ground; however higher altitude observations are also permitted.

- f. Irradiance of the Sun: The source code uses the transmission coefficient (determined by running the LOWTRAN6 program) multiplied by the irradiance existing at the top of the atmosphere to yield the radiance at the cloud.

### 3. Computer Model for the Cloud Radiance

This is a program for the 3 to 5 micrometers wavelength region which calculates the cloud signature and makes estimations for the expected signal range value [Ref.16]. Other calculated factors are the atmospheric transmission coefficient using the LOWTRAN6 program, the solar radiation scattered by the various cloud and atmospheric scenes and finally the spectral response of the instruments. Further explicit calculations include the scattering of the sun rays according to various geometric aspect views (top, bottom, left and right views). For this purpose the Monte Carlo statistical method [Ref.18] has been implemented since it is the only one with the desired flexibility to be applied to every cloud scene. In addition to the Monte Carlo approximations multiple expansions are used including the doubling method [Ref.17] and the two

stream diffusion models for radiation transport [Ref.19] for the n-stream approximations.

The main problem of the previously mentioned approximations is with the realistic three dimensional cloud scenes. These problems are partially solved, as described in chapter 3 of this thesis, by tracking the scattering of the individual photons for various scattering phases with the obvious disadvantage of spending too much computer time since the number of tries for different photons is high.

In the more specific case where approximated values for the radiance model are needed the number of trial photons can be reduced. Further indication of the accuracy of the calculations is provided by the program by giving the statistical uncertainties according to the viewing geometries and the scattering model.

By combining different functions such as the spectral scattering albedo, the solar spectral irradiance, the scattered signatures spectral bandpass, the instrument bandpass, the spectral emissivity and finally the Lowtran transmittance the in-band intensity can be calculated. The selection of the wavelength for each photon in the scattering process can also be determined by obtaining the spectral weighting function after combining the instruments components and the solar transmittance.

## B. CODE DEVELOPMENT

The present version of the BMAP is the initial edition which is based on the modeling of a structured infrared cloud background according to various atmospheric conditions and infrared local scenes. Future editions of the BMAP will be based on the development of a cloud structure model which will be accessed according to the meteorological conditions for the local area of observations. This structural model will be in conjunction with the frequency and spatial characterization which will be accessed through statistical correlation as shown in Figure 4.1 [Ref.16]. The reason that this can be done is that we can parameterize a cloud structure with respect to its infrared image in terms of various parameters such as spatial frequencies, edgeness, contrast, etc.

This can be done by building a data bank of the above mentioned parameters for different meteorological conditions at the exact moment of observation of the data and in such a way that an immediate correlation can be made between the input conditions and the data. For this to be achieved several cloud images must be analyzed, stored and correlated.

Finally all that the user will have to do is to input the local conditions of observation which will be combined with the spatial characteristics for the infrared scene, and a map of the cloud with the correct structural features will be produced.



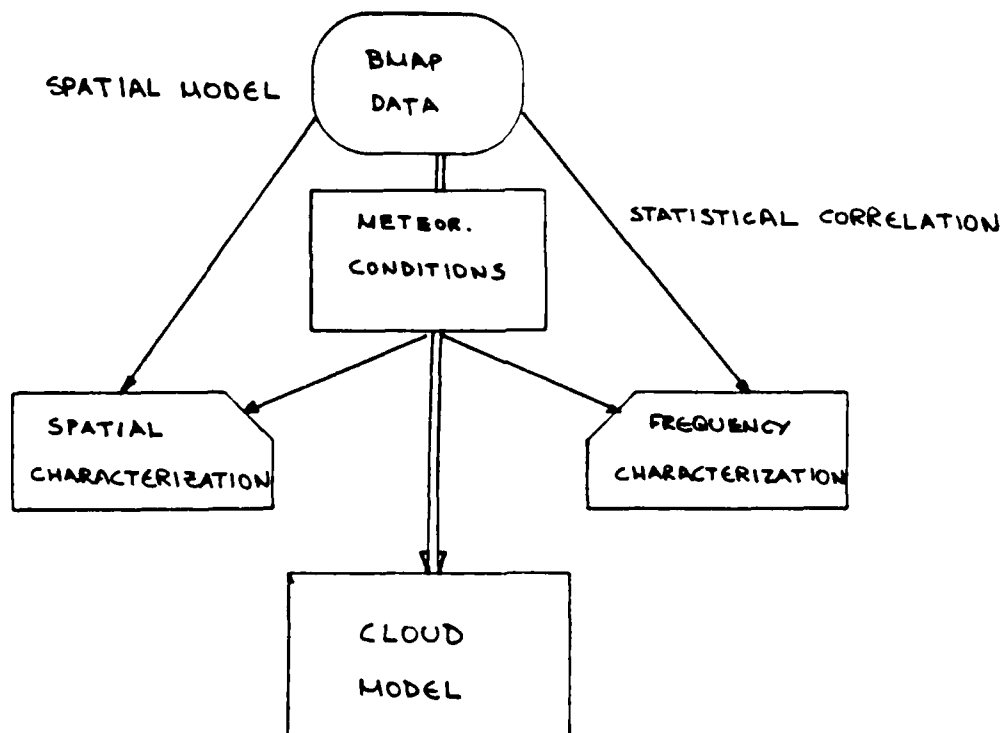


Figure 4.1 Structural outline of the BMAP program

### C. LOWTRAN6 PROGRAM

There are three sub-programs inside the BMAP program which can be accessed through the function keys of the main code, as will be explained in chapter 5 of this thesis, or can be run individually as independent programs from the directory.

The LOWTRAN6 is a Fortran program which is designed to calculate radiance and atmospheric transmittance  $\tau(\lambda)$  averaged over  $20 \text{ cm}^{-1}$  in steps of  $5 \text{ cm}^{-1}$ . The atmospheric transmittance [Ref.1] can be expressed as:

$$\tau(\lambda) = e^{-\tau(\lambda)R} \quad (4-1)$$

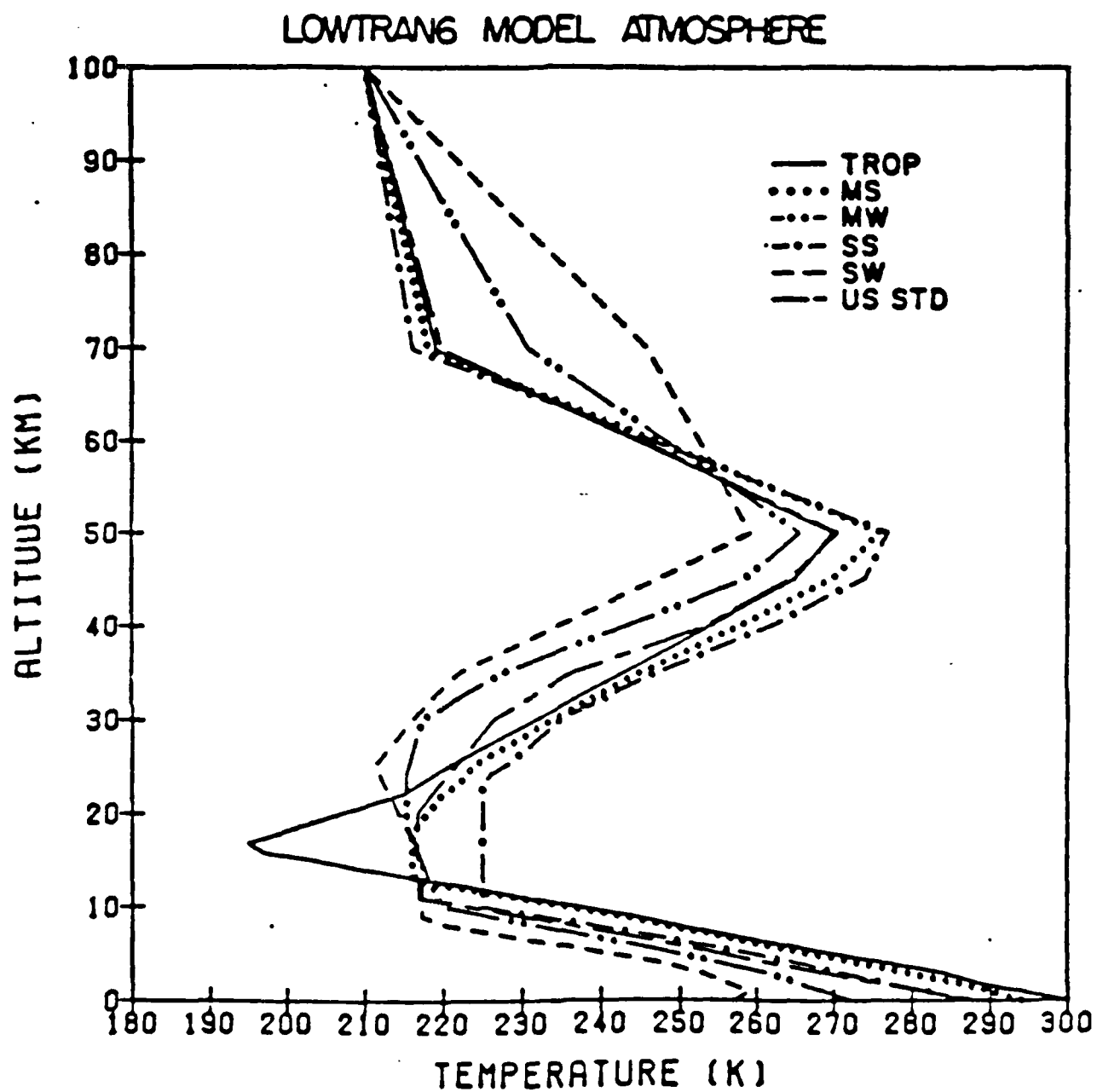


Figure 4.2 Various Atmospheric models in use with the LOWTRAN6 code (From Ref.4).

where  $r(\lambda)$  is the extinction coefficient (equal to the sum of the scattering coefficient  $\tau(\lambda)$  and the absorption coefficient  $\sigma(\lambda)$ ) and  $R$  is the range.

For the BMAP code further development of the LOWTRAN code include calculation of the transmission of Solar Irradiance and of the radiance with or without scattering present.

In the model we have a single parameter band model for molecular absorption. The code also includes the continuum absorption in the 3 to 5 micrometers band by the water vapor and the nitrogen and the absorption in the 8 to 12 micrometers band by the water is included in the code. These two atmospheric windows in the infrared are caused not only by the water but also by other absorbing gases like carbon dioxide (2.7, 4.3, 15 micrometers), the ozone (4.8, 3.2, 6.3 micrometers) and the nitrogen. Nitrogen absorption has its greatest value in the 8 to 14 micrometers region.

In the code the earth's curvature and the refraction have also been taken into consideration.

In the propagation code the atmosphere consists of 33 layers with variable width (1 Km up to an altitude of 25 Km, 5 Km up to an altitude from 25 to 50 Km, from 50 to 70 Km, and from 70 Km to 100 Km). The user has the choice of 6 atmospheric models [Figure 4.2] which are the 1962 US Standard model, the Mean Tropical model, the Mid Latitude Summer model, the Mid Latitude Winter model, the Sub-Arctic Summer model and finally the Sub-Arctic Winter model.

Furthermore the user has the choice of six aerosol models; these are the Rural model with visibility 5 Km, the Rural with visibility 23 Km, the Maritime model with visibility 23 Km, the Navy Maritime model with variable visibility, the Urban model with visibility of 5 Km, the Tropospheric model with visibility 50 Km and finally a user defined model with visibility 23 Km. A major difference from the LOWTRAN6 program in the IBM 3033 computer of the Naval Postgraduate School is that the Advection fog and the Radiation fog models in use are not incorporated in the BMAP program.

For the rain cases the rain-induced extinction coefficient has been defined by the Mie Scattering theory and the Marshall-Palmer raindrop size distribution [Ref.4]. Appendix A of this thesis includes a table of the cards used by the BMAP LOWTRAN code. Further information about the structure of these models and about the mathematical definitions governing the transmission inside each of these models is not within the scope of this thesis but it can be found in detail in References 4 and 15.

## V. COMPUTER CODE FOR CLUTTER - KEY FUNCTIONS

### A. GENERAL

The BMAP program is a code designed to operate in a small IBM portable AT computer using the INTEL 80287 math co-processor chip and the Tecmar high resolution graphics card with an optional hard disk and a 9 track tape drive.

The code comes with three BMAP Bedford files named BEDFORD1, BEDFORD2, BEDFORD3, each 12160 bytes long, which can be accessed from the program using the F1 key.

All of the data and the text input are accomplished using the computer keyboard (standard type) with certain tasks done by the arrow and function keys.

The computer code has a variety of capabilities which can be accessed using either the keyboard or a penpad digital tablet or a combination of them. The future user can find more detailed information in reference 16 about the use of the keyboard or the penpad.

The source code has three main options which are represented by three sets of icons. These sets are the DISPLAY module, the ANALYSIS module and the MODELING module. A summarized description of these modules is presented in figure 5.1 [Ref.16]. Each module set consists of a variety of icons which always appear on the left side of the screen in a manner corresponding to the F1...F10 keys of the keyboard.

These modules have one thing in common regarding the

CODE CAPABILITIES			
<u>MODULE</u>	<u>ICON NAME</u>	<u>DESCRIPTION</u>	<u>PRINTER OUTPUT</u>
DISPLAY <sup>1,4</sup>	Data Select	Access icon set to display new data	
	Cursor	Puts cursor on the screen & prints row, column & pixel value	
	Threshold	Changes the range of pixels displayed	
	2D Plot	Generates an on-screen plot of a BMAP channel	X
	3D Plot	Generate an onscreen 3D surface plot in 4 perspectives	X
ANALYSIS	Histogram	Displays a histogram of the BMAP image	
	Edge <sup>2</sup>	Computes & displays edge operators on BMAP image	X
	Metrics <sup>2</sup>	Computes passive image metrics	X
	2D PSD	Computes 2D PSD of data	X
	Filter	High & low pass PSD filter & inverse 2D FFT to compute a filtered image	
MODEL	Signal Processing	Access icons for signal processing	
	Spectral <sup>3</sup>	Computes Monte Carlo radiance model	
	Spatial <sup>2</sup>	Model cloud spatial structure	
	Lowin	Generates Lowtran input & graph file	
	Lowtran	Lowtran 6	
	Lowplt	Outputs Lowtran graph	X

Figure 5.1 Summary of DISPLAY, ANALYSIS and MODELING modules  
(From Ref.16)

function keys. The F1, F3, F5, F10 keys have the same function no matter what module is running at the moment and are:

F1: Gets the DISPLAY module

F3: Gets the ANALYSIS module

F5: Gets the MODELING module

F10: Exits the program and returns the user to DOS

The functions of the rest of the buttons for each module are presented in Appendix C of this thesis.

## B. COMPUTER MODULES

### 1. Display Module

This module appears on the computer screen when the program is loaded and consists of the infrared image on the top of the screen with an empty space below (in which the different program options appear with a set of icons having the following functions/capabilities:

- a. Icon 1 (F1 key): We have No change since the DISPLAY module is already present.
- b. Icon 2 (F2 key): Allows the user the selection of a new image and returns him to the data directory icons.
- c. Icon 3 (F3 key): Brings the ANALYSIS module on screen.
- d. Icon 4 (F4 key): Creates a cursor on the infrared image on the top of the screen which will provide

data information about the specific point under the cursor. The data is presented under the image first by the number of the channel which that point represented when the data was taken, then the sample number and finally the radiance (number of counts).

- e. Icon 5 (F5 key): This key brings up the MODEL module.
- f. Icon 6 (F6 key): This key makes the adjustment in the range of the count values on the display which is usually within some specific range of values. The program asks the user for an upper and a lower threshold value for the new range which will improve the ability to redistribute the shades of gray in the new range and to improve the clarity in the picture of the image.
- g. Icon 7 (F7 key): When this option is selected the program provides a two dimensional plot of one channel only. In the beginning the user must provide the code with the channel number (from 1 to 16) that he wishes to plot. Then the program will provide the counts for the required channel and a plot of the sample. Each count signifies radiance of  $5.6 \times 10^{-8}$  watts/cm<sup>2</sup>-steradian. In Figures 5.2 and 5.3 [Ref.16] we have a representation of the channels #2 and #6 of the BEDFORD1 file.
- h. Icon 8 (F8 key): This key will give the counts versus samples for all of the 16 channels and a three



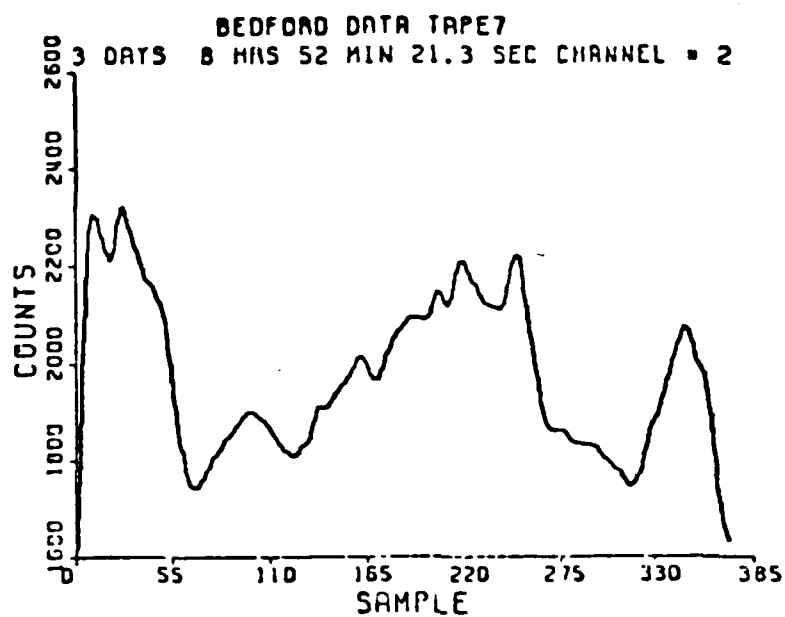
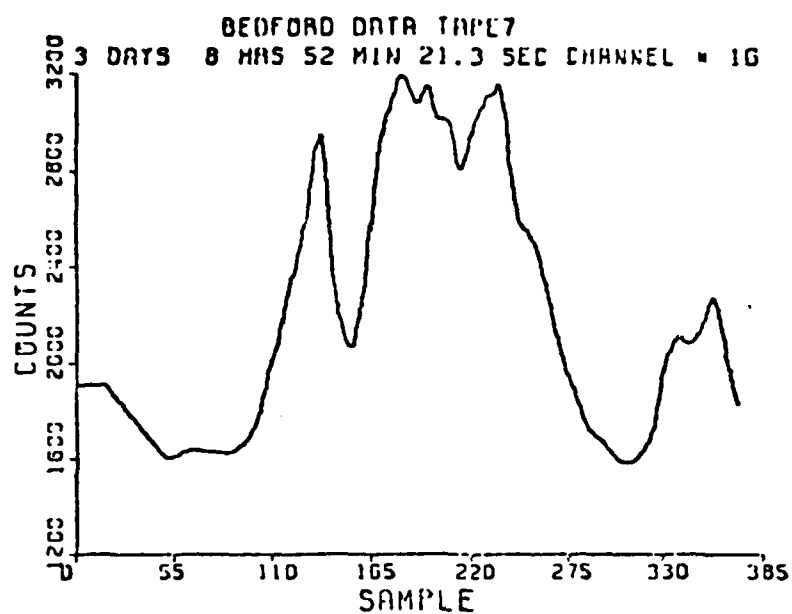


Figure 5.2 Two dimensional plot for channel #2 of BEDFORD1  
(From Ref.16)



1 count =  $5.6 \times 10^{-8}$  watts/(cm<sup>2</sup> - steradian)

Figure 5.3 Two dimensional plot for channel #6 of BEDFORD1  
(From Ref.16)

3 DAYS 8 HRS 52 MIN  
21.3 SEC

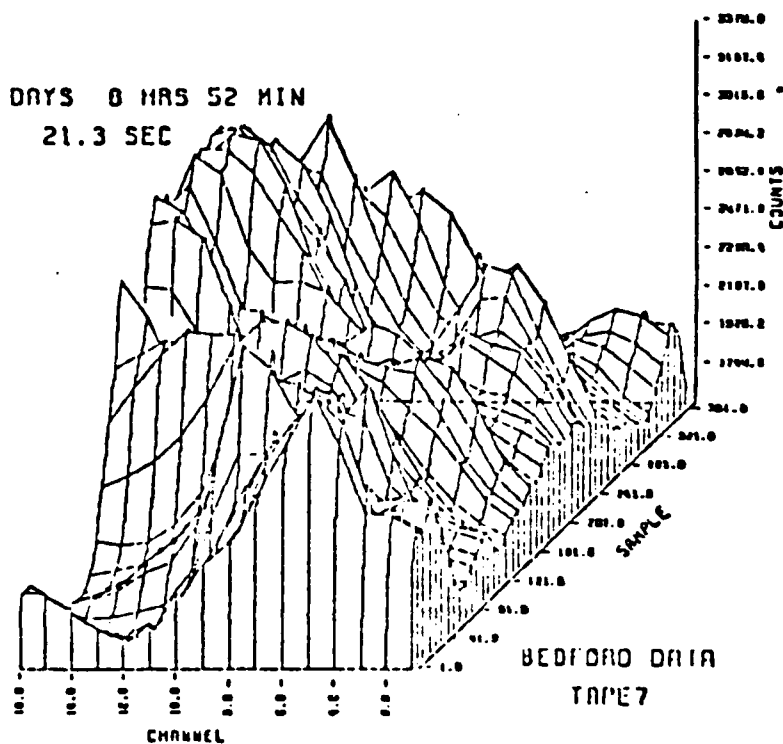


Figure 5.4 Three dimensional plot of BEDFORD1 file  
(all 16 channels), (From Ref.16)

dimensional plot of the image, and provides the user with different options regarding the way the plot is to be observed (view aspects). These options are front to back, right to left, left to right and finally back to front. Figure 5.4 [Ref.16] gives the three dimensional plot of the BEDFORD1 file for all 16 channels.

- i. Icon 9 (F9 key): This key will give the directory of the disk and is similar to the DOS command "Directory".
- j. Icon 10 (F10 key): This key exits the program and returns to DOS.

## 2. ANALYSIS module

This is the module that provides modeling of the data and various cloud scenes with the option to present and filter the power spectral density (PSD) of an image. This module consists of 10 icons with the following functions:

- a. Icon 1 (F1 key): Brings the DISPLAY module and its functions on the screen.
- b. Icon 2 (F2 key): This function will give a histogram of an image with the number of counts on the bottom of the screen. (The vertical direction signifies the number of pixels for the specific count value.
- c. Icon 3 (F3 key): This brings up the ANALYSIS module and its functions on the screen.

- d. Icon 4 (F4 key): This function is intended for future use with the revised edition of the BMAP and will compute and display the edge operators for an infrared image.
- e. Icon 5 (F5 key): This brings up the MODEL module and its functions on the screen.
- f. Icon 6 (F6 key): This function is also intended for future use in the revised edition of the program and will compute passive image metrics.
- g. Icon 7 (F7 key): This will compute a two dimensional power spectral density (2D-PSD) for an infrared scene and display it on the screen. This is done by first calculating the Fast Fourier Transform of the image, if this has not already been done, and then presenting it on the screen in a logarithmic or linear scale according to the user's wish. In the case that the linear scale is chosen as an option a further option of clipping the DC value is available. In Figure 5.5 [Ref.16] we have a two dimensional plot of BEDFORD1 file with the vertical axis representing the power spectrum (linear scale), the horizontal axis the sample counts and the transverse axis the channel number.
- h. Icon 8 (F8 key): This function will provide filtering of the power spectral density and then display it on the screen by first computing the Fast Fourier

Transform of the image and then filtering according to the cutoff index. Four types of filtering are available:

1. In the sample direction / High pass filtering
2. In the sample direction / Low pass filtering
3. In the channel direction / High pass filtering
4. In the channel direction / Low pass filtering

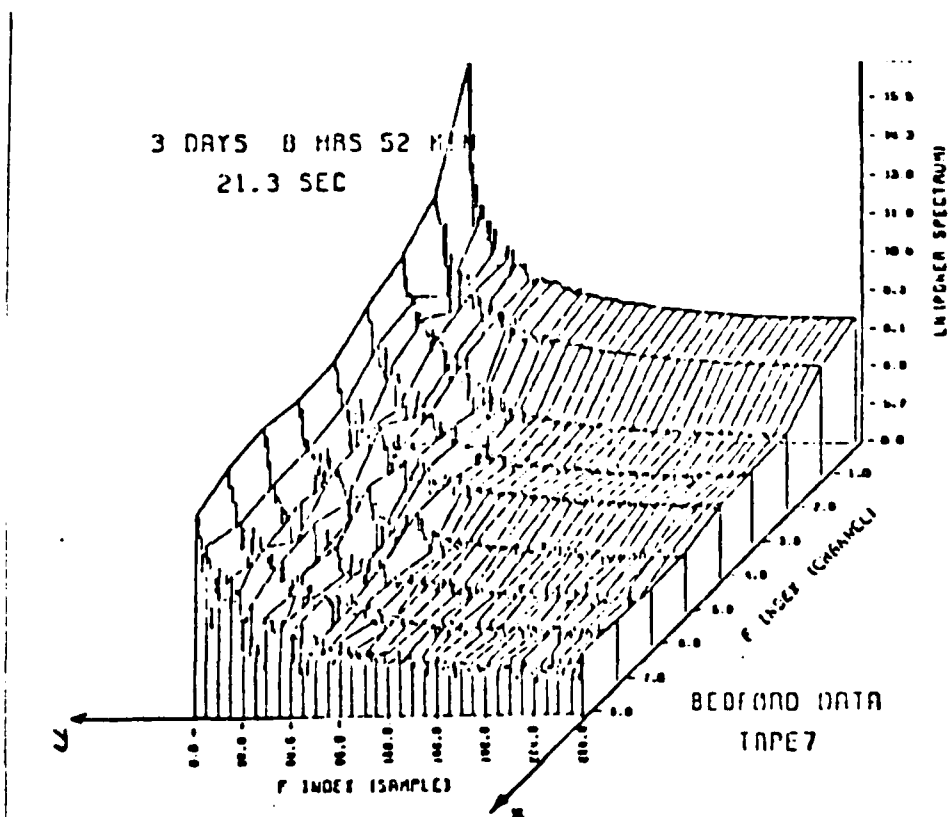


Figure 5.5 Two dimensional plot of BEDFORD1 file for power spectrum (From Ref.16)

When the filtering is occurring in the channel direction the cutoff index can be a channel from 1 to 8. When the filtering is in the sample direction the cutoff index is a sample number.

The roll off coefficient C then must be inserted found from the formula [Ref.16]:

$$\text{Roll off} = e^{-D^2/C} \quad (5-1)$$

where D=distance from the cutoff, and

C=roll-off coefficient.

This will give the rate with which the signal falls off after the cutoff.

The previously mentioned filtering techniques can be used individually or all together. Then the program will perform the inverse Fast Fourier Transform of the image and will display it on the screen.

Icon 9 (F9 key): This option is intended for future use and will access further icons from the code for signal processing.

- j. Icon 10 (F10 key): Exits the program and returns the user to DOS.

### 3. MODELING module

This module of the BMAP calculates the radiance using the Monte Carlo method, previously described in chapter 3 of this thesis, and the reflected and transmitted intensity for each cloud layer in a cloudy infrared scene. A further option

of this module includes the LOWTRAN6 code with its accompanying subprograms LOWIN and LOWTRAN plotting. More in detail the module consists of the following icons:

- a. Icon 1 (F1 key): Brings up the DISPLAY module and it's icons on the screen.
- b. Icon 2 (F2 key): This function will compute the radiance model using the Monte Carlo statistical method model. That model uses values taken from the LOWIN subprogram which can be changed according to the desire of the user. That means that the LOWIN and LOWTRAN programs must have been run ahead before the radiance is calculated. Otherwise the values for the Monte Carlo statistical method analysis will be from a previous run and the results will be wrong. The spectral modeling icon then will calculate the reflected and transmitted intensity for each cloud layer. It must be noted though that this function is yet not fully implemented.
- c. Icon 3 (F3 key): This brings the ANALYSIS module and its functions on screen.
- d. Icon 4 (F4 key): This is intended for future use in the revised edition of the BMAP and will give a cloud model Spatial Structure.
- e. Icon 5 (F5 key): Brings the MODEL module and its functions on the screen.



- f. Icon 6 (F6 key): This function is the Lowin subprogram for the LOWTRAN6 program. Its use is to insert the values required to run the LOWTRAN program and the LOWPLOT program. This subprogram consists of 4 cards, presented in Appendix A. Further explanation of the function of these cards and the various variables that can be inserted can be found in the Chapter 4 of this thesis and in Ref.15.
- g. Icon 7 (F7 key): This option will use the values which are assigned to the Lowin subprogram (icon 6) and run the LOWTRAN program. More details about the LOWTRAN6 program can be found in Chapter 4 of this thesis and in Ref 15.
- h. Icon 8 (F8 key): This option will give the output LOWTRAN plots. When this function comes to the screen it will present a card, an example of which is presented in Appendix A, with different variables according to the type of lines that are going to be used in the plots. More details can be found in Ref.15.
- i. Icon 9 (F9 key): This will bring up the directory from the disk and it has the same function as the "Directory" command of DOS.
- j. Icon 10 (F10 key): This will exit the code and return the user to DOS.

As a general remark for all modules it should be noted that a help routine is always available to the user which can be accessed by pressing the <Alt> key in conjunction with one of the F1...F10 keys. The code then will give a short description in the function of the specific key.

## VI. BMAP TAPE FORMAT

### A. GENERAL

The BMAP code consists of three data files called BEDFORD1, BEDFORD2, BEDFORD3 with the name originating from the place of data measurement on top of a hill at an elevation of 250 feet above mean sea level in Bedford, MA from 10 to 14 September 1984.

The experiments were made with the participation of NSWC, NADC, NRL and the Raytheon Corporation in a hole in a solid cloud deck in the sky that was backlit by the sun. The sensor was a Raytheon dual band scanning radiometer in the wavelength spectrum from 4 to 5 and from 8 to 11 micrometers. The sensor had two 16 element arrays with an instantaneous field of view (IFOV)  $0.33 \times 0.33$  millirad and Total Field of View (TFOV)  $16 \times 512$  pixels. It must be noted that the arrays were boresighted and calibrated with reference to a two temperature internal blackbody standard.

### B. INTERNAL CONFIGURATION

#### 1. Introduction

The BEDFORD data files are arranged according to an interactive computer code called ATITP based on the NRL code 6520 implementation of the NATO standard Image transfer [Ref.24] requirements. The computer code gives as an output a

9 track magnetic tape which can be used for infrared data interchange.

The NRL code 6520 is a VAX/VMS 11 disk structure which will be imposed with an internal file structure in such a way that the information can be transferred to a 9 track magnetic tape for further data manipulation. Its purpose is to enable the various users to access the data inside the NRL magnetic tapes.

The BEDFORD files in the BMAP are arranged in the same way in a format consisting of three parts as in Figure 6.1 [Ref.24].

The first part has the name "Header 1" and is a record of the source of the file data BEDFORD files and a brief description of the data in part two and three. "Header 1" also gives information about the origin of the files, the data organization and the structure of the files in a standard format.

"Header 1" consists of three basic parts. The first part consists of the bytes from 1 to 24 identifying the origin of the image. The second part consists of the bytes from 25 to 80 giving a description of the rest of the data in the file. The third part uses the bytes from 81 to 104 giving information about the x and y sizes and the type of the data. Finally we have the bytes from 105 to 128 which are unassigned at present and will be used for expansion and

modification for future versions of the code by specifying multi-image files.

The second part has the name "Header 2" and is a tape record of the structural detail of the data following in part three.

With "Header 2" we can have free format documentation of all the necessary parameters for the data such as the location of the significant image features and documentation relating the recording environment.

It must be noted that at the end of each header there follows an "End of File" (EOF) mark which usually creates a problem since it makes each header a separate file, consequentially making the main file (BEDFORD file) unreadable without some special decoding technique. The problem can be eliminated by ignoring the headers and skipping the first two records providing, of course, that we know the image data structure that follows.

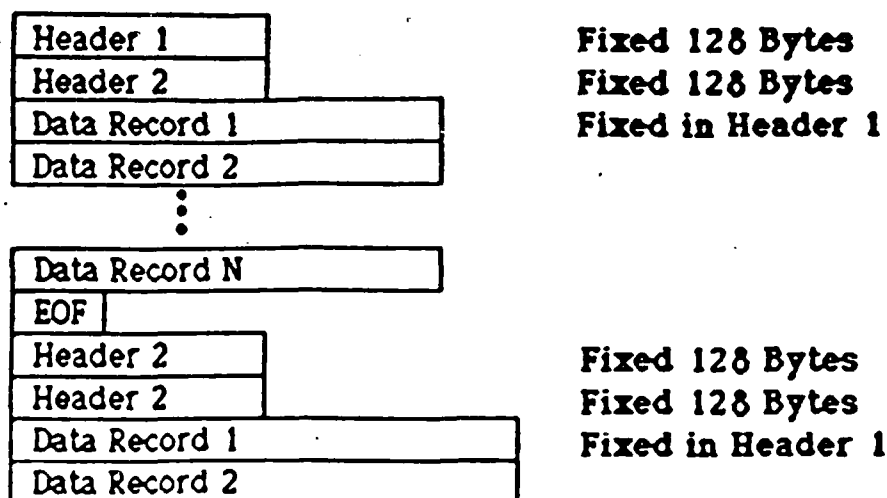


Figure 6.1 BEDFORD files byte structure (From Ref.16)

The data file representing each image in the tape record differs in form from the organization of pixel data recorded from the measurements sensor [Ref.25]. Thus we can have each image written on the tape as a separate file without necessarily having each record containing one image line. The form of this configuration permits the user to use the format to transfer very long image lines (16 channels for the BEDFORD files images) using a small tape buffer size of 4K existing in small computers, such as the IBM AT, and in mini computers, such as the Masscomp computer of the IRSTD

U	S	A		N	R	L	
8	5			3		2	8
T	A	P	E	7	C	A	L
						1	8
					1	2	8
							2
							1
							2
							0
							0
						1	6
							0

ORIGINATOR CODE  
DATE TAPE MADE  
NRL INTERNAL FILE IDENTIFIER  
NUMBER OF RECORDS IN FILE  
SIZE OF FILE 2  
TWO BYTE INTEGER VALUES  
ONE ENTRY PER SAMPLE  
TWO BYTES PER "CHANNEL"  
REAL MANTISA BYTES (UNUSED)  
REAL EXPONENT BYTES (UNUSED)  
SAMPLES PER LINE  
LINES PER IMAGE  
NONCOMPLEX INTEGER DATA  
16 UNUSED BYTES.

Figure 6.2 BEUFORD file Header 1

From 1965 to 1970

The basic format of the data is based on the tape character (byte). The same format can be used for 7 track tape as 6 bits and in 9 track tape, as for the BEDFORD files, at 8 bits.

## 2. Structure of "Header 1"

The "Header 1" field consists of 128 bytes in 16 eight byte fields in a configuration according to Figure 6.2 [Ref.24].

"Header 1" for a 7 track tape is coded in BCD code even parity and for a 9 track tape in ASCII code odd parity.

In the "Header 1" we can find the following information:

<u>Bytes</u>	<u>Presenting Information</u>
1 to 8	Identity of the originator with 4 symbols for the country and 4 symbols for the laboratory
9 to 16	Date of data Year, Month, Day
17 to 24	Name or number of file, image, or program units
25 to 32	Number of records per file. R = R-NUM * 1000000 for a Header record
33 to 40	Number of tape characters in Header 1, 2, 3, 4 with the tape character
41 to 48	Number of tape characters in Header 1, 2, 3, 4, 5 with the tape character
49 to 56	Number of tape characters in Header 1, 2, 3, 4, 5, 6 with the tape character
57 to 64	Number of tape characters in Header 1, 2, 3, 4, 5, 6, 7 with the tape character
65 to 72	Number of tape characters in Header 1, 2, 3, 4, 5, 6, 7, 8 with the tape character
73 to 80	Number of tape characters in Header 1, 2, 3, 4, 5, 6, 7, 8, 9 with the tape character
81 to 88	Number of tape characters in Header 1, 2, 3, 4, 5, 6, 7, 8, 9, 10 with the tape character
89 to 96	Number of tape characters in Header 1, 2, 3, 4, 5, 6, 7, 8, 9, 10, 11 with the tape character
97 to 104	Number of tape characters in Header 1, 2, 3, 4, 5, 6, 7, 8, 9, 10, 11, 12 with the tape character
105 to 112	Number of tape characters in Header 1, 2, 3, 4, 5, 6, 7, 8, 9, 10, 11, 12, 13 with the tape character
113 to 120	Number of tape characters in Header 1, 2, 3, 4, 5, 6, 7, 8, 9, 10, 11, 12, 13, 14 with the tape character
121 to 128	Number of tape characters in Header 1, 2, 3, 4, 5, 6, 7, 8, 9, 10, 11, 12, 13, 14, 15 with the tape character

complex data are treated as two channel data with  $C=2 \times \text{number of channels}$ )

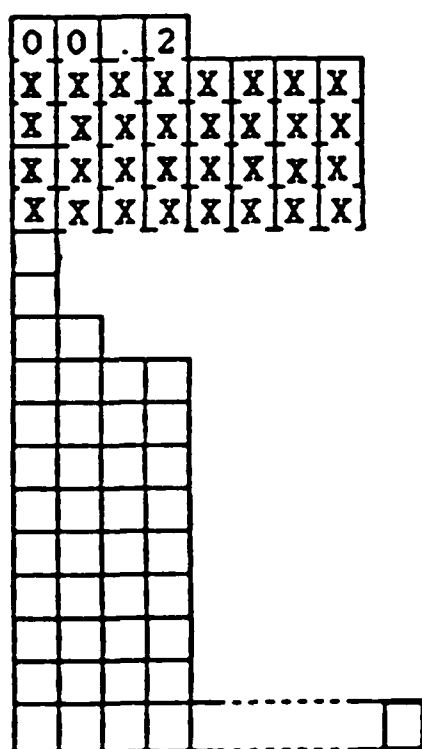
57 to 64	Number of tape characters per channel for integer data (I) or Number of card images on the file (I=0 for real values)
65 to 72	Number of tape characters for mantissa of a real valued channel ( $E_m$ ) ( $E_m=0$ for integer values)
73 to 80	Number of tape characters for exponent of a real valued channel ( $E_e$ ) ( $E_e=0$ for integer values)
81 to 88	Number of samples per line (S)
89 to 96	Number of lines per image (L1)
97 to 104	Type of data values (T) with: T=0 for non-complex, integer T=1 for complex, integer T=2 for non-complex, real T=3 for complex, real T=4 for source code card images (80 characters per source code line)
105 to 128	Currently not assigned

### 3. Structure of "Header 2"

The file Header 2 in its structure defines a series of fields containing ASCII character strings taking advantage of the fact that the length of the ASCII standard format is 128 characters. The fields are as follows:



The "Header 2" configuration contains a description of the image including the physical significance of the various channels, meteorological conditions of the day when the data were taken, description of the scanner used, location of objects in image, etc. Its length is variable between 0 and 4096 characters [Ref.25] and has the same coding as the "Header 1".



**L1 TRUE IF LONG WAVE DATA**  
**L2 TRUE IF MID WAVE DATA**  
**I2 CORRECTION PGM. CODE**  
**I4 CORRECTION PGM. VERSION**  
**I4 VAX DATA FORMAT**  
**I4 FIRST CHANNEL OUTPUT**  
**I4 LAST CHANNEL OUTPUT**  
**I4 FIRST EVEN DATA POINT**  
**I4 LAST EVEN DATA POINT**  
**I4 FIRST ODD DATA POINT**  
**I4 LAST ODD DATA POINT**  
**64 BYTES FOR FUTURE**  
**EXPANSION**

Figure 6.3 BEDFORD "Header 2" configuration (From Ref 16)

In the file the first 4 bytes are used to specify the header version number which can always be changed according to whether new information has been added or removed. At present the version is 00.2. The next field is 32 bytes long and is used to specify the time at which the data were taken. We then have two 1 byte logical fields that signify the wave band of the data. If the letter "T" is on the third field then the data are longwave (8-12 micrometers). If on the other hand the letter "T" is on the fourth field then the data are midwave (3-5 micrometers). For the BEDFORD files the letter "T" is on the fourth field.

The next bytes are used for file correction. According to NRL standards the usual method of doing the correction of a file is by using two data correction programs called "CORRECTIN" and "ERRFND" [Ref.24]. The program used is symbolized in the "Header 2" file in the next field by the two digit code "1" if the correction program is the "CORRECTIN" and the two digit code "2" if the correction program is the "ERRFND". For better insurance the version number of the correction program is stored in the next four bytes position.

The next field, four bytes long, is used to store the tape data version number from which the data were taken. The next six fields are four bytes long and are used to store the location of the data in the file. The first two fields are used to store the location of the data in the file and the next two fields are used to store the location of the data in the file.

output, first even data point, last even data point, first odd data point, and last odd data point. Finally the last 64 bytes are used for future expansion.

#### 4. Data structure

The data inside the BEDFORD files are stored in fixed length records the number of which can be found from information given by the 'Header 1'. For the BEDFORD files, Figure 6.2, the number of records is 18. In each record we have one scan line of data. That means that for the 18 records we have 18 scan lines of data for each BEDFORD file. The image data are binary odd parity and one's complement [Ref.25] in integer format which remains the same for all of the other types of format as described in 'Header 1' configuration for the bytes 97 to 104. In the integer format the most important part is recorded as a first tape character with the most significant bit (the farthest left) being the sign bit 0 for positive and 1 for negative.

For the real format the exponent and the mantissa which are base 2, are reduced to integers and are then stored as separate integers. For each sample in the tape, for the complex format the integer and the real parts of the complex number are stored as integers and the real and imaginary parts are stored as real numbers. For the real format the real and imaginary parts are stored as real numbers. For the complex format the integer and the real parts of the complex number are stored as integers and the real and imaginary parts are stored as real numbers. For the real format the real and imaginary parts are stored as real numbers. For the complex format the integer and the real parts of the complex number are stored as integers and the real and imaginary parts are stored as real numbers.

part and each sample consists of 2 channels (2 real and 2 imaginary parts).

The NRL data banks have various infrared images in NATO standard format in various computer formats like the following cases.

In the case of multi-channel data the register and the non-register parts are stored as separate images in separate files.

Another method for the multi-channel case is to store the data on a pixel interleaved basis and to remove the values of the different channels as adjacent bytes for one sample as in Figure 6.5. This figure shows storing methods for three color non-complex data and two channel complex data.

#### 2 channel, complex data

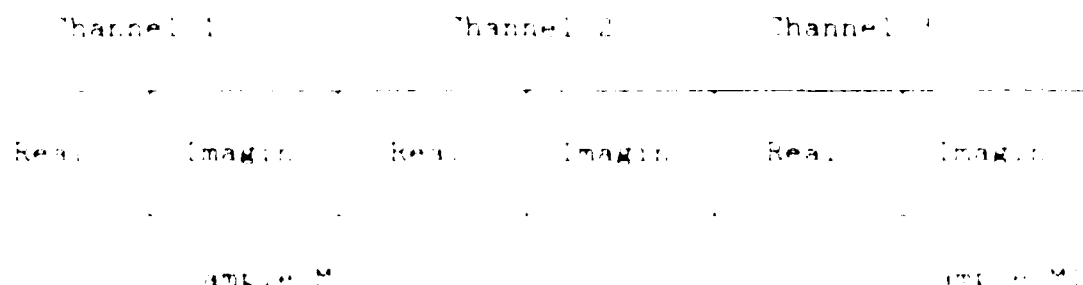


Figure 6.5: Storing methods for three color non-complex data

Figure 6.5: Storing methods for three color non-complex data

Figure 6.5: Storing methods for three color non-complex data

is the same as the two's complement since all data are of reasonable magnitude and positive.

In Figure 6.6 [Ref.24] we have a representation for the data format structure of the BEDFORD files.

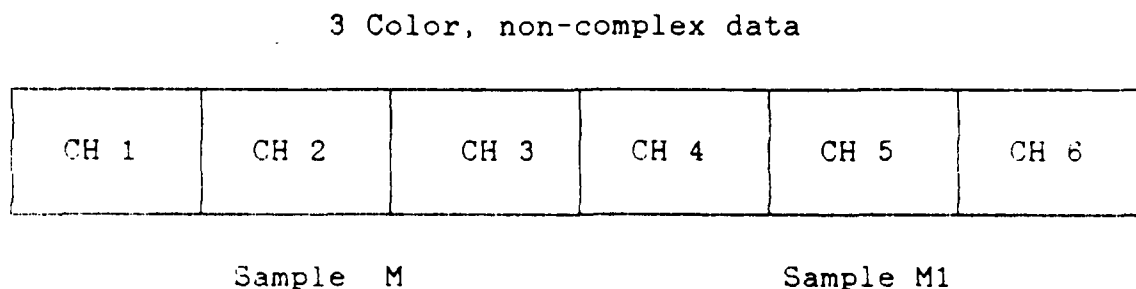


Figure 6.5 Multi-channel data storing methods

At the end of the tape a marker <END OF FILE> is placed signifying the end of the data records. After that a new tape with data records can be added. The final end of the tape is marked with two markers <END OF FILE>.

#### 5. Physical Interpretation of the data

The BEDFORD files data were taken, as already described in the previous chapter, using a sensor consisting of two bore sighted telescopes measuring intensity. In front of each telescope there was an optical bandpass filter covering the eight to sixteen infrared detectors. These detectors were connected to a computer system which processed the data and stored it in the BEDFORD files. The data were then used for the analysis of the infrared radiation emitted by the objects in the field of view of the telescopes.

response with a 0.5-1000 Hz and 3 db passband. The electronic bandpass of the second one was 0-1000 Hz at 3db [Ref.26].

Each telescope scanned across  $2.2^\circ$  of azimuth with a speed of  $36.0^\circ$  per second and for a scan time of 60 seconds. The intensity then was sampled every 0.096 mR which created 300 data points per scan. It must be noted that the sampling time was less than the dwell time and since the angular resolution was 0.33 mR that creates 3.44 intervals of 0.096 mR per dwell.

For each detector the random noise level was 2.5 mV. For that reason the data digitization was from 0 to 11 (12 bits) (0-4096 decimal) so that each count was also 2.5 mV. The random noise error was 2-3% since the maximum relative intensity variations spanned about 50 counts.

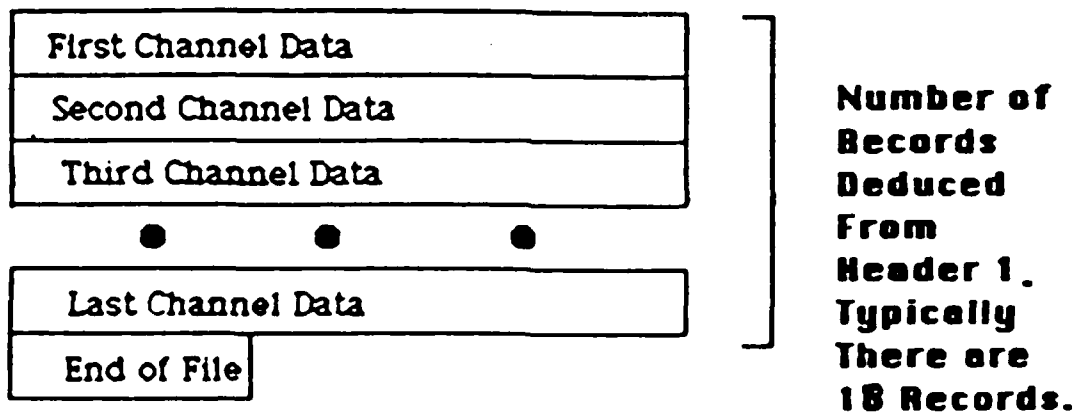


Figure 6-6 Data structure format of BEEP RI files

From Ref. 18

## VII. AGA DATA FORMAT

### A. GENERAL

The AGA Thermovision 780 is a thermographic device with digital recording and data analysis capabilities able to detect infrared radiation in the middle infrared spectrum (3-5 micrometers) and/or the far infrared spectrum (8-14 micrometers) using an InSb detector for the first and a HgCdTe for the second. Further information about the AGA system can be found in the AGA manual in Reference 28.

The AGA is connected to a micro-computer of West German origin, BMC IF 800 model 20, which uses a Z-80, 4 MHz clock microprocessor and a CPM operating system.

The computer operates with a software package consisting of three major programs called DISCO, IMAGE PROCESSING and UTILITY which interface with the AGA Thermovision 780 and record infrared Images in a 16 bit word form on a diskette in one of the systems drives [Ref.28].

### B. IMAGE/DATA TRANSFER

The infrared image in data form can be transferred at any point from the diskette into a RAM inside the computer for further processing.

The user though must write a program in either BASIC or PASCAL provided that they are installed into the BMC

computer) and call a subroutine from the DISCO diskette called REDA.

The subroutine REDA is written in assembly language and its purpose is to transfer an infrared image from the data diskette to RAM memory inside the computer as an 8192 or 16384 pixel file, depending whether the form of the image is FIELD or FRAME [Ref.27]. Each image inside the RAM will occupy 8192 or 16384 bytes accordingly with a 77 16-bit word directory data. The number of images that can be transferred depends exclusively on the size of the RAM.

The image is then stored as a matrix of 128 elements (width) by 64/128 elements (height) in a sequential method starting from the left hand corner of the image and passing from the end of the first line restarting at the left most image point at the second line of the image.

The REDA subroutine can be called by writing inside the user's program:

```
"call REDA (Param1, Param2, Param3)"
```

where Param1 is an integer from 1 to 38 corresponding to the image number, Param2 is also an integer corresponding to the address of the first element of the image directory data and Param3 is a single byte integer corresponding to the first pixel of the image buffer.

The infrared image in the RAM can be read by the program starting the initial data and the parameters of the image from which the image was read. The program can also read the



disk	1	1	1	ascii	1	high and low byte holds each
label	1		1		1	1 ascii
im.no.	1	2	1	16 bit int	1	image number
	1		1		1	
RANGE	1	3	1	16 bit int	1	
LEVEL	1	4	1	16 bit int	1	
	1		1		1	
abs(A)	1	5,6,7	1	24 bit int	1	$\text{abs}(A) = 65536 \cdot \text{DI}(5) + 256 \cdot \text{DI}(6) + \text{DI}(7)$
B	1	8	1	16 bit int	1	
abs(C*1000)	1	9,10,11	1	24 bit int	1	$\text{abs}(C) = (65536 \cdot \text{DI}(9) + 256 \cdot \text{DI}(10) + \text{DI}(11)) / 1000$
	1		1		1	
Dcal*10	1	12	1	16 bit int	1	calibration distance (m)
	1		1		1	$\text{dcal} = \text{DI}(9) / 10$
sign (A,C)	1	13	1	16 bit int	1	bit 0: sign of C
	1		1		1	bit 1: sign of A
	1		1		1	
EPS*100	1	14	1	16 bit int	1	emissivity obj. * 100
DIS	1	15	1	16 bit int	1	object distance (m)
Tamb*10	1	16	1	16 bit int	1	ambient temperature (K) * 10
Tatm*10	1	17	1	16 bit int	1	atmospheric temperature (K) * 10
TRMS*100	1	18	1	16 bit int	1	transmission * 100
alpha*100000	1	19,20,21	1	24 bit int	1	$\alpha = (65536 \cdot \text{DI}(19) + 256 \cdot \text{DI}(20) + \text{DI}(21)) / 100000$
	1		1		1	
beta*100000	1	22,23,24	1	24 bit int	1	$\beta = (65536 \cdot \text{DI}(22) + 256 \cdot \text{DI}(23) + \text{DI}(24)) / 100000$
	1		1		1	
D/R sw	1	25	1	16 bit int	1	direct/relative switch
	1		1		1	1: relative, 0: direct
EPSR*100	1	26	1	16 bit int	1	emissivity ref., $\text{epsr} = \text{DI}(26) / 100$
XR	1	27	1	16 bit int	1	horizontal position ref.
YR	1	28	1	16 bit int	1	vertical position ref.
VALR	1	29	1	16 bit int	1	digital value of reference point
Tref*10	1	30	1	16 bit int	1	reference temperature (K) * 10
	1		1		1	
SCY	1	31	1	16 bit int	1	scanner type
SCVER	1	32,33,34	1	ascii	1	scanner version
SERNO	1	35	1	16 bit int	1	serial no.
FILCOD	1	36,37,38	1	ascii	1	filter code
FOV*2	1	39	1	16 bit int	1	fov DI(39)/2
APERT*	1	40	1	16 bit int	1	aperture, $\text{ap} = \text{DI}(40) / 10$

Figure 1: BEA data structure for the 16 bit version of the BEA-16 bit version

directory of each image will be stored inside the RAM from the REDA subroutine is presented in Figure 7.1.

With the use of the REDA subroutine the user can connect the data generated by the AGA Thermovision 780 with other processing software like the IBM operating BMAP program.

The main problem is the incompatibility of the 16 bit image of the AGA to the 8 bit image of the BMAP program and the difference in the data format. Further discussion of the differences is presented in Chapter X of this thesis.

NO-A191 135

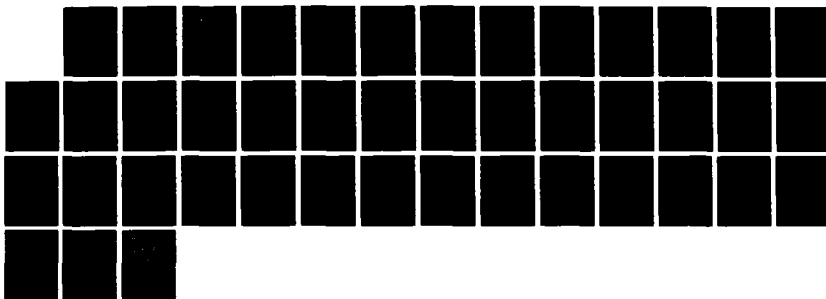
SKY RADIANCE DISTRIBUTIONS FOR THERMAL IMAGING  
BACKGROUNDS(U) NAVAL POSTGRADUATE SCHOOL MONTEREY CA  
A KOTSIS DEC 87

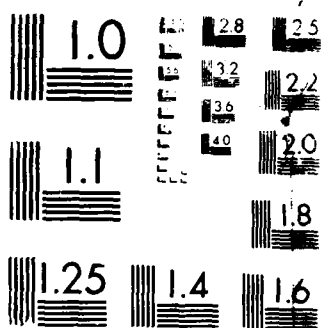
2/2

UNCLASSIFIED

F/G 4/1

ML





## VIII. DATA PROCESSING IN THE IRSTD SYSTEM

### A. GENERAL

The NPS-IRSTD data processing system is based on the initial version of the system the IRST (Infrared Search and Track System).

The IRST is a system with automatic detection capability for infrared targets provided to the system from the Electronic Processing Equipment (EPE) after the necessary clutter rejection (which is the lower blue sky target signal insertion loss with a corresponding high clutter rejection), in conjunction with synthetic display capability on a real time basis.

The EPE consists of the following components [Ref.22]:

- a. Signal Processing Subsystem (SPS) with sub-components:
  - 1. Background Normalized Unit (BNU)
  - 2. Signal Buffer and Power Supply Unit (BPU)
  - 3. Data Conditioner Unit (DCU)
- b. Data Processing Subsystem (DPS) with sub-components:
  - 1. Running software
  - 2. DPS hardware
- c. Display and Control Subsystem (DCS).

### B. INTERNAL CONFIGURATION OF THE IRST/IRSTD SYSTEM

#### 1. Signal Processing Subsystem

The Electronic Processing Equipment Unit presented in 8.1 and 8.2 with its subordinate units, a full description of

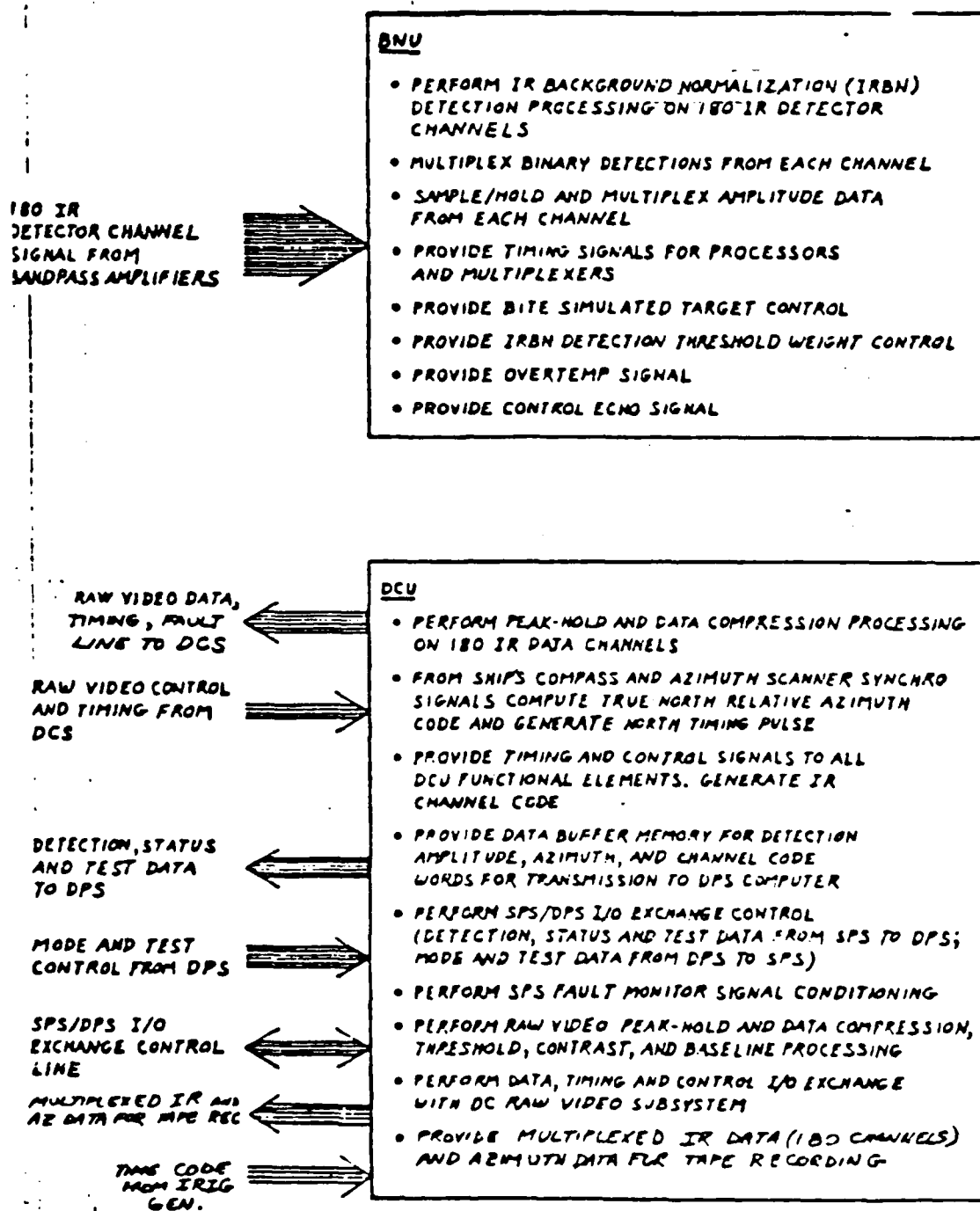


Figure 8.1 Signal Processing Subsystem Layout 1

(From Ref.22)

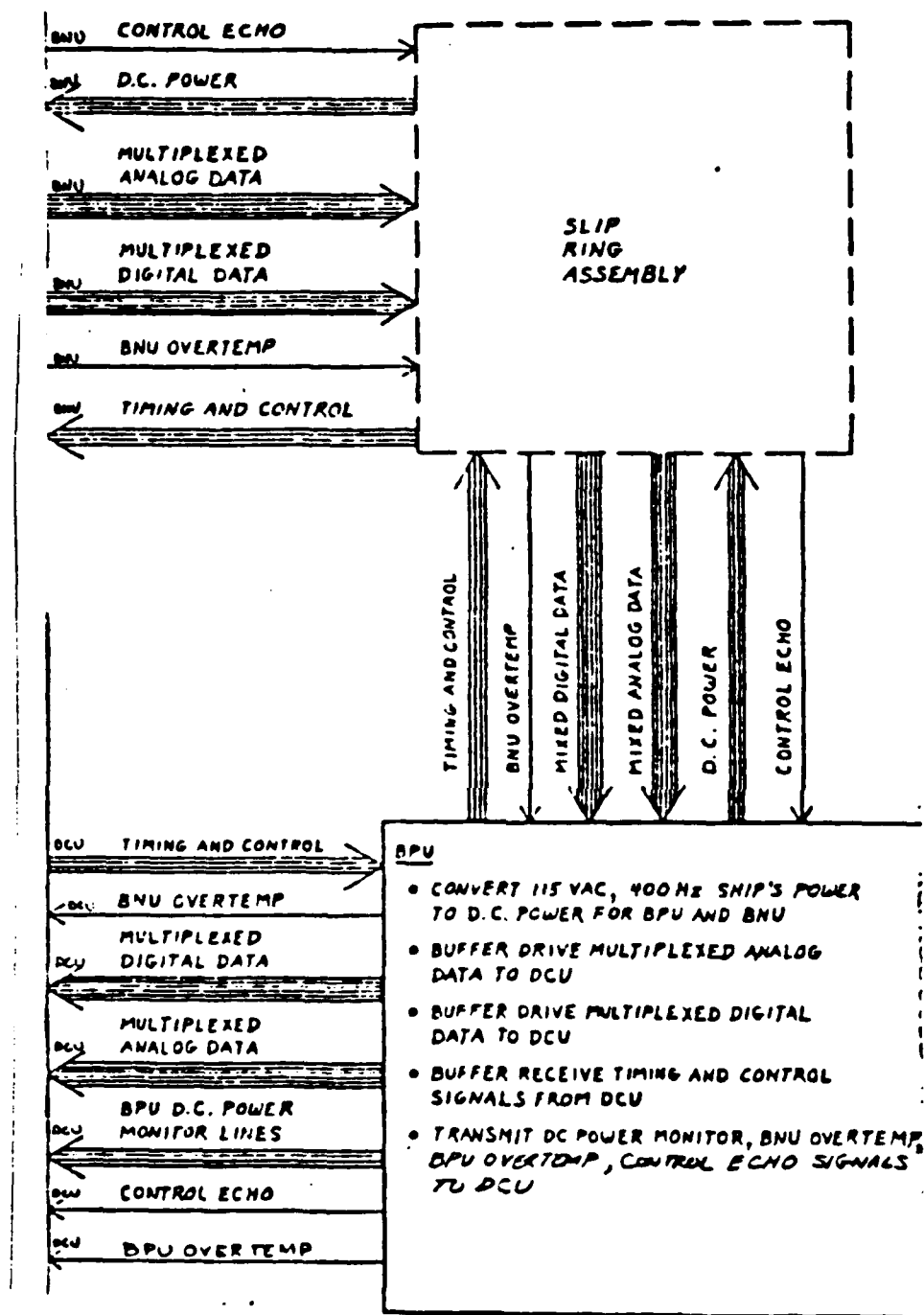


Figure 8.2 Signal Processing Subsystem layout 2

(From Ref.22)

which is given in the IRST manual in Ref.22, receives a pre-processed raw video from the optics, spectral filters, cold stop, detectors, pre-amplifiers and bandpass filters through 180 detector channels from the scanning infrared optical unit. These channels come from two 90-detector linear arrays (in the image plane) separated by a  $1/2$  degree, which are spectrally filtered in different wavelength bands. The existence of the two arrays ensures the coverage of the specified elevation angle with a total field of view of  $360^\circ$  in azimuth.

These detector channels (180 total) providing the raw video coming from the detector's pre-amplifiers and bandpass filters interface with the Signal Processing Subsystem and are filtered through a technique which keeps the specified per scan constant false alarm rate (CFAR) with a corresponding low target insertion loss. The normalized detector channel data are then synchronized by the SPS unit with the corresponding coordinate data so the Data Processing Subsystem data are buffered, digitized and formatted.

## 2. Data Processor Subsystem

The unprocessed video after the Signal Processing Subsystem goes to the Data Processor Subsystem (DPS) where a further correlation/track and target discrimination is been performed so the IRST false designation requirement is maintained. Further on the DPS unit keeps the tracking of all the pre-designated targets and reports the track status on



the Display and Control Subsystem in the form of target amplitude, target coordinates and detection array number. An additional ability of the DPS unit includes reporting and target designation through the NTDS system of the home platform.

### 3. Display and Control Subsystem

This subsystem provides the necessary control of the IRST system by displaying both the unprocessed and the processed video in conjunction with the system status. Further on the system provides identification of any track as a noise or clutter track, target designations, blanking zone capability, scan false alarm rate control and other track store information according to the user's request. More information about the DCS unit can be found in Ref.22.

### 4. Data Processing

The data processing functions are performed by the AN/UYK computer of the IRST system and by the Masscomp computer of the IRSTD system with its software with the following modes of operation [Ref.22]:

- a. Data Input (for reporting detections)
- b. External Function (for control of the computer)
- c. Interrupt Input (for the time code to the computer, ships heading, and reporting of the system status)
- d. Data output (for the testing of the Data Conditioner Unit functions).

## C. DATA CONFIGURATION

### 1. Introduction

This is the mode in which the signal processor target detections will be input. The input data consists of two words, each with a length of 16 bits for the IRST system and of 12 bits for the IRSTD system, which will be transferred in parallel for each message. For the 16 bits case of the IRST system each input consists of 8 bits for the amplitude, 1 bit for the array number, 7 bits for the channel number (elevation information), 14 bits for the azimuth degrees and the rest are control bits [Ref.22]. The memory words will be transferred to the Data Conditioner Unit with a maximum rate of 900 KHz.

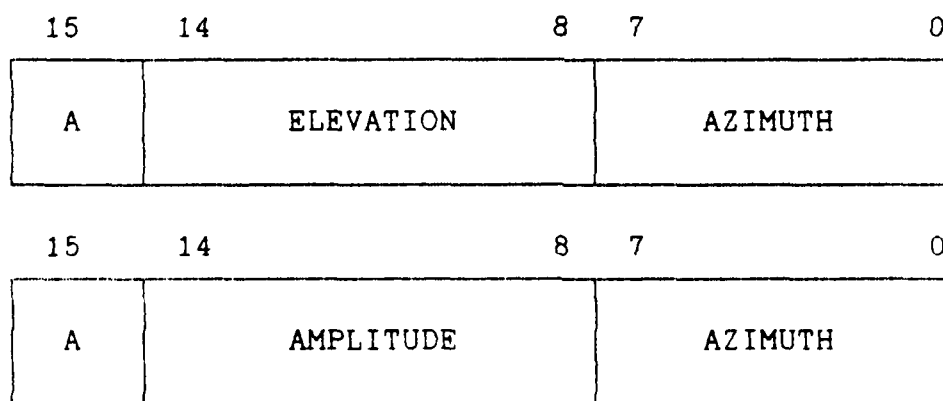


Figure 8.3 Format of the 16 bits words input to the DCU

The threshold settings though will be less than 1K words/second with a maximum peak rate of 50K words/second. In Figure 8.3 [Ref.22] we have the information format of the two 16 bit words.

Where:        A. Array designation with 0=leading and  
                 1=trailing

ELEVATION. Detector number from 0 to 89

AMPLITUDE. Detection Amplitude Magnitude

AZIMUTH. Azimuth counter value at the time of the  
                 report to the Data Processor

E/F. Empty/Full indicator with 1=Empty and 0=Full

The input queue will be 1024 words in a circular buffer which will permit a maximum of 512 two-word unprocessed reports to be queued before an overflow happens. The 16 bit format though in the IRSTD version will be used for testing purposes only. The actual format will be in the 12 bits word versions where the 1 to 8 bits will be used for the Analog to Digital Convertors (ADC) of the IRSTD (12 ADC's x 15 max.=180 channels) and the remaining 4 bits in each word will be used for position, frame and rotation synchronization.

## 2. Synchronization and Geometry of the Data

The IRSTD data coming from the optical sensor unit can be considered to be an array of 180 rows (representing 180 channels) by 60,000 columns (representing 360 degrees coverage of the optical sensor).

The data coming from the sensor will then go to the Masscomp computer in a form of stream of data words, each word representing a data value for each of the 180 sensors in the IRSTD scanner unit. That data stream will then be



more specifically the determination of where the boundaries of the array will be.

The first problem will be solved by controlling the data, forcing them to have the correct rate and input timing by synchronization of the data stream. This synchronization will be made by two leading bits in the beginning of each word. In such a way the software of the Masscomp computer will be synchronized with the optical scanning unit.

The first bit will be set to the "one" state at the beginning of the rotation of the optical unit and then to "zero" state for the period of time that the rotation is being made.

The second bit will be set to one for the first 180 sensors and to zero for the next 179 sensors. With the help of the first leading bit the Masscomp computer will be first synchronized with the optical unit and then will start reading the data until the second bit changes value, meaning that the first 180 sensor values have been read and transferred to the Masscomp computer.

The second problem will be solved by buffering the data stream in two separate buffers. In that way when one buffer is filling with the incoming data, the next buffer will be available for storing and processing of the data into the magnetic tape drive of the IRSTD processing system. The data will be parallel input into the buffer every synchronized clock pulse as presented in Figure 8.5.



## IX. DATA ANALYSIS

### A. GENERAL

In this chapter we will discuss the way the data from the BEDFORD1 to BEDFORD3 files are decoded from their original form to alpha-numerical form and then how the data of which they consist were transferred to three output files called BEDFORD1.OUT, BEDFORD2.OUT, and BEDFORD3.OUT. Finally we will discuss how these output files were transferred to the Masscomp computer of the NPS-IRSTD system.

We will also discuss the method in which the decoding computer code was developed explaining each component of the code in detail.

### B. COMPUTER CODE ANALYSIS

#### 1. Introduction

As it was already explained in Chapter V of this thesis the BEDFORD files consist of two header form of information followed by a matrix of integer data. Each header consists of two 128 byte alpha-numerical (character) strings with special and specific details about the data that follow in an integer matrix of infrared information in integer\*2 form.

The whole infrared image, represented by the data matrix, consisted of 16 lines of 371 data points making a total of 5936 data points.

At the beginning of the code analysis an attempt was made to read the data by conventional methods by examining each file with the DOS command "BROWSE".

The attempt was unsuccessful due to the fact that the data in the BEDFORD files were encoded. A computer program in an advanced language was required that could read that data. We then contacted the ONTAR company, which developed the BMAP program to explain the coded form of the data and a possible way to decode the data. The ONTAR company responded by sending some information about the form of the headers and a computer code written in Microsoft Fortran which they claimed could read the data. The ONTAR computer code is presented in Appendix D.

We then tried to use the ONTAR code to read the BEDFORD files but with unsuccessful results since the Microsoft Linker running the ONTAR computer code could not recognize the functions "OPENFH", "RDEMEM", "IADDRS" and "CLOSFH" found in the code.

The ONTAR company was contacted once more and asked for the above mentioned functions. They responded to us saying that these functions are proprietary to the company and they could not be given to us. This response made the code provided by them unusable. Another method had to be found to read the data from the BEDFORD files. That method was to develop our own computer code in RM/FORTRAN that would be able to read the BEDFORD files and extract the data so they



could be later on transferred to the Masscomp computer of the IRSTD.

## 2. Code Analysis

A program written in RM/ FORTRAN can read a data file written in one of the following forms:

1. FORMATTED files consisting entirely of formatted records.
2. UNFORMATTED files consisting entirely of unformatted records.

The way these files are accessed/addressed determines how the records are read or written from a file. Furthermore, depending on the order in which the data are arranged inside the files, we can have sequential or direct access. The sequential files contain no logical gaps, can vary in length and can contain an End of File record. The direct access files can either be written or read in any order since they are random access files and they have a record number identifying the logical position of the record in the file.

Our first attempt was to read the BEDFORD files using the sequential access method. The reason we did this was that by using a utility program (Norton Utilities) we recognized End of Files markers between the data (ASCII characters 1A and 1D) which looked like Figure 9.1.

Our attempt was unsuccessful due to the fact that, although the beginning headers are formatted in sequential records of 128 bytes each, the following data are records not

having a specific length but rather varying in length for every line representing a separate detector as described in Chapter V.

The formatted method caused the integer data to be read as formatted characters instead of integers. For that reason every time an attempt to compile the program was made we encountered an error "-1" meaning that an "End of File" was encountered on the reading attempt.

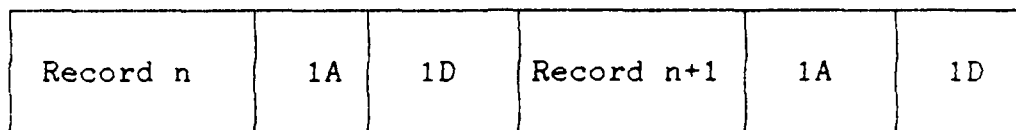


Figure 9.1 Formatted Sequential Data

We changed the method of accessing the data to the Unformatted Sequential method with unsuccessful results once more due to the fact that the data records this time were not sequential.

We then tried the Unformatted Direct Access method and once more we had unsuccessful results. But this time there was no error in the method but we had an oversight error. When we opened the file as a direct formatted access record we should assign a record length defined by the "RECL" specifier in the open statement. The "RECL" specifier was first set to one so we would be able to read the header characters one at a time. However the data matrix following

was in integer\*2 format and trying to read that format one byte at a time made the attempt unsuccessful.

The problem was solved by opening the file once by using record length equal to one (RECL=1) in order to read the headers and then, after closing the file, re-opening it again using a record length equal to two (RECL=2). The reason we did this was to bypass the problem of the integer\*2 of the data so the computer could read them. The file was opened by using as a dummy argument the file's name (BEDFORD1, BEDFORD2, BEDFORD3). The format was "Unformatted", the status of the file was "OLD" and the file access was "DIRECT". More information about the code is presented in Appendix B.

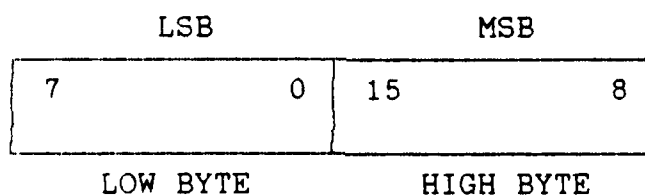


Figure 9.2 DOS data SWAP for integer\*2 data

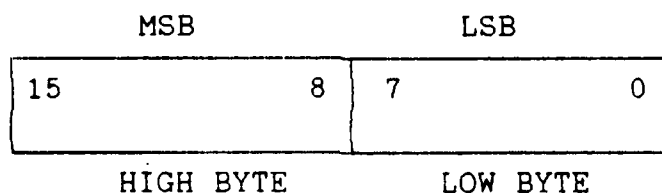


Figure 9.3 BMAP data SWAP for integer\*2 data

We then had another problem to solve. The data were encrypted in the DOS basic coding for the integer\*2 format

presented in Figure 9.2 with a small alteration. That alteration was that the most significant byte and the least significant byte were interchanged as presented in Figure 9.3.

The Fortran program in Appendix B uses a subroutine called "SWAP" to achieve this. What that subroutine does is to reverse the order of bytes and replace the least significant byte with the most significant byte.

Finally after this problem was solved the data were read successfully and were transferred into three output files called "BEDFORD1.OUT", "BEDFORD2.OUT" and "BEDFORD3.OUT".

We then used a normal modem communications program between computers called "PCTALK 4" to transfer the three files to the Masscomp computer of the NPS-IRSTD system.

## X. CONCLUSIONS AND RECOMMENDATIONS

### A. CONCLUSIONS

The BMAP program is a program with analysis, modeling and plotting capabilities of various infrared background scenes. It is created in support of the NSWC clutter computer code originally designed for the Navy's fleet defense systems and especially for analyzing a target's background signature against a clutter background.

The program was initially provided with three background infrared scenes called BEDFORD 1, 2, 3, which are typical representatives of the NATO Standard Format of recording and storing infrared scenes.

We evaluated the BMAP program to find out its capabilities. The program proved to be excellent in analyzing and modeling the infrared data of the provided files with the program. For the analysis it used 2D Fast Fourier Transform comparison and other processing techniques, a version of the LOWTRAN propagation code and high resolution graphics for the screen including excellent plotting in a normal printer. We then evaluated the AGA DISCO program of the IF 800 computer and discovered a subroutine called "REDA" which can be used to transfer the AGA infrared image file data to the IF 800 memory and then by writing another computer code in BASIC or FORTRAN to transfer the same data to the IBM AT computer.

We evaluated the present data file form of the NPS/ IRSTD MASSCOMP computer for use of the BMAP program with a future application of transferring the data from the AGA through the IBM AT computer to the masscomp.

We then attempted to transfer the three data sets from the BMAP program to the Masscomp computer. It must be mentioned that the BMAP program is not limited to only the three BEDFORD data sets. It can also be used with all the data sets, now currently available from the Naval Research Laboratories, describing various infrared atmospheric scenes. Since these files are recorded and stored in the same method and format as the BEDFORD files it is assumed that the BMAP program will be able to perform its powerful capabilities with these files too.

These data sets now can be transferred to the Masscomp computer of the IRSTD for further processing in conjunction with incoming data from the IRSTD sensor now on its final engineering development. In such a way we will be able to combine the infrared target picture of the IRSTD with one of the infrared background scenes that will be stored inside the Masscomp computer of the IRSTD.

For being able to do this we had first to transfer the BEDFORD files (typical Nato Standard Format infrared scenes) from the compatible IBM AT computer to the Masscomp computer. These files were first coded in a format described in the previous chapters which did not permit their transfer in an

understandable form. A computer algorithm had to be made that would be able to decode the data in to a simple alpha-numerical format that would be able to be transferred to the Masscomp computer with a modem.

We then developed a computer software program in RM/FORTRAN, as described in Chapter IX and Appendix B, which was able to decode the BEDFORD files and rewrite them into three output files in alpha-numerical form.

The output files created under this program were then transferred to the Masscomp computer using a modem and a simple software transferring program called "PC-TALK 4" for internal storage and further processing with the IRSTD infrared data.

## B. RECOMMENDATIONS

Since we know that the Naval Research Laboratories have a great variety of infrared background scenes written according to the BMAP/BEDFORD format we recommend that these files be obtained for further analysis using the BMAP program. In that way we will not only explore the NRL computer library of infrared scenes but will also create one of our own with the same data on the IBM compatible computer.

It is then recommended that these infrared scenes be transferred to the Masscomp computer of the IRSTD, using the same developed RM/FORTRAN algorithm for further processing with the IRSTD data.

A further development of this thesis will be the transfer of infrared scenes from the small portable AGA Thermovision 780 system to the Masscomp computer. To do this it is recommended that a computer code be written in BASIC or FORTRAN calling the "REDA" subroutine in the IF 800 computer to read the infrared scenes of the AGA (already in storage in diskettes) in to memory. They can then be transfered to the IBM compatible AT computer using the "REDA" subroutine, as described in Chapter VII, and then, using the RM/FORTRAN algorithm, transfered to the Masscomp computer for further processing .

By doing this we should be able to make a comparison of the infrared scenes obtained with the AGA and with the IRSTD to make a rough estimation of what the IRSTD is really seeing and improving the capabilities of both systems



# APPENDIX A

## LOWTRAN (LOWIN-LOWPLOT) INPUT FILES

Model Atmosphere	Meteorologic Data
Type of Atmospheric Path	Horizontal Path
Mode of Execution	Transmittance
Temperature & Pressure Altitude Profile	
Water Vapor Altitude Profile	
Ozone Altitude Profile	
Radiosonde Data are to be Input	No
Supress Profile Output	No
Temp at Boundary (.000 - T @ 1st level)	.000
Surface Albedo (.000 - Blackbody)	.000
Extinction Type & Default Range	No Aerosol Attenuation
Seasonal Arosol Profile	Determined by Model
Aerosol Profile & Extinction Type	Background Stratosphric
Air Mass Character	0
Inclusion of Cirrus Attenuation	No
Use of Army (VSA) for Aerosols	No
Surface Range (.000 - Default)	.000
Current Wind Speed (m/sec)	.000
24-Hr average Wind Speed (m/sec)	.000
Rain Rate (mm/hr)	.000

Plot Type	Transmittance cm <sup>-1</sup>
Type of X Axis	Linear
Type of Y Axis	Linear
Number of Decimal Digits for Y Axis	1
Length of X Axis (in inches)	7.0000
Beginning Wavenumber/Wavelength	2000.0000
Ending Wavenumber/Wavelength	4000.0000
X Axis Annotation Interval	400.0000
Length of Y Axis (in inches)	6.0000
Minimum Transmittance/Radiance	.00E+00
Maximum Transmittance/Radiance	.00E+00
Y Axis Annotation Interval	.00E+00
Altitude (km)	.000
Pressure (mb)	.000
Ambient Temperature (degrees)	.000
Dewpoint Temperature (degrees)	.000
Relative Humidity (%)	.000
Water Vapor Density (gm/m3)	.000
Ozone Density (gm/m3)	.000
Path Length (km)	.000
Initial Frequency (wavenumber)	2000.000
Final Frequency (wavenumber)	4000.000
Frequency Increment (wavenumber)	5.000

## APPENDIX B

### RM/FORTRAN COMPUTER CODE TO EXTRACT THE DATA FROM THE BEDFORD FILES OF THE BMAP SOURCE CODE

c this program reads files partially successfully if they  
c are at least 30 lines long  
\* this subroutine reads a matrix  
\* RFILE has been changed to read binary rather than formatted

\* variable names

\* FILENAME name of data file  
\* X 1st variable  
\* Y 2nd variable  
\* Z 3rd variable  
\* NPTS number of data points

\* inputs

character filename\*8,var\*1,array(256)\*1

\* outputs

real\*4 x(6000)

\* local

logical here,there,everywhere

integer Inunit, errorfile, j, k,npts,ival(10),l,i,s

integer\*2 data,cdata,bpdata(5936)

character infile\*8, dummy\*10

```

        print *, 'Input filename to open  '
        read(6, '(a8)') filename

*
* Assign the unit number
        Inunit = 9
100 format(I8)
c   print *, 'input record length'
        s=0
        j=1
        print *, 'j=  '.j
        open(unit=2, file='bedford.out')
* open file
        infile = filename
        open  (unit=Inunit,
:           file=filename,
:           iostat=errorfile,
:           status='old',
:           form='unformatted',
:           access='direct',
:           recl=j)

        if (errorfile.ne.0) then
        print *, 'Error opening ', filename
        close (Inunit)
        go to 1000
        end if

        inquire(file=filename,

```

```

:      iostat=ios,
:      exist=here,
:      opened=there,
:      access=dummy)
print *, 'filename,ios,exist,opened,access'
print *, filename,ios,here,there, ' ', dummy

* read heading
88  continue
    k=256
c   print *, 'input value of record length of header'
c   read (6,100) k
    print *, 'read ival from Inunit '
    print *, ' '
    do 77 j=1,k
        read(inunit,rec=j) var
        array(j)=var
        write (6,200) var
        write(2,200) var
200 format(\a1)
77  continue
    print *, 'rewrite'
    write (6,*) array
    close(Inunit)

```

```

c read data

c  print *, 'input record length of data-'
c  print *, '      (i.e., number of bytes per data point):'
c  read (6,100) j
      j=2
      print *, 'j= ', j
* open file
      infile = filename
      open  (unit=Inunit,
            :      file=filename,
            :      iostat=errorfile,
            :      status='old',
            :      form='unformatted',
            :      access='direct',
            :      recl=j)
            if (errorfile.ne.0) then
              print *, 'Error opening ', filename
              close (Inunit)
              go to 1000
            end if

c  print *, 'input starting data address'
c  read (6,100) j
      print *, ' '
      do 5 l=1,5936
        read(inunit,rec=l+128) data
        call swap(data,cdata)

```

```

        if (cdata .lt. 0) s=s+1
        bpdata(1)=cdata
5      continue

c      print data
      do 6 i=0,5935,11
      write(6,300) bpdata(i+1),bpdata(i+2),bpdata(i+3),
        . bpdata(i+4),bpdata(i+5),bpdata(i+6),bpdata(i+7),
        . bpdata(i+8),bpdata(i+9),bpdata(i+10),bpdata(i+11)
c      . ,bpdata(i+12),bpdata(i+13),bpdata(i+14),bpdata(i+15)
        write(2,300) bpdata(i+1),bpdata(i+2),bpdata(i+3),
        . bpdata(i+4),bpdata(i+5),bpdata(i+6),bpdata(i+7),
        . bpdata(i+8),bpdata(i+9),bpdata(i+10),bpdata(i+11)
6      continue
300     format(1x,15(I5,1x))
        print *, s, ' negative numbers in data'

1000    close (Inunit)
        stop
        end
        subroutine swap(b,c)
        integer*2 b,c
        c=ishc(b,8)
        return
        end

```

## APPENDIX C

### KEY FUNCTIONS FOR THE BMAP PROGRAM

#### DISPLAY MODULE

F2 key \*\*\*\*\*  
Brings the DISPLAY MENU model  
and:  
Data Select  
Cursor  
Threshold Image  
2D Plot  
3D Plot  
DIR  
Exits the Program

F2 key \*\*\*\*\*  
Gets a new set  
of images.

F3 key \*\*\*\*\*  
Brings the ANALYSIS MENU model  
and:  
Histogram  
Edge Operators  
Image Metrics  
2D PSD  
Filter PSD  
Signal Proc.  
Exits the Program

F4 key \*\*\*\*\*  
Points and  
reports pixel  
values.  
Terminates  
with the ESC key.

F5 key \*\*\*\*\*  
Brings the MODELLING MENU model  
and:  
Monte Carlo  
Structure Model  
LOWIN  
LOWTRAN 6.1  
LOWPLT  
DIR  
Exits the Program

F6 key \*\*\*\*\*  
Changes the thresholds



for the image display  
F7 key \*\*\*\*\*  
2D Plotting  
F8 key \*\*\*\*\*  
3D Plotting  
F9 key \*\*\*\*\*  
Allows the  
examination of  
a directory  
during program  
execution.  
F0 key \*\*\*\*\*  
Stops program  
execution and  
returns to DOS.

## MODEL MODULE

F1 key \*\*\*\*\*  
Brings the DISPLAY MENU module  
and:  
Data Select  
Cursor  
Threshold Image  
2D Plot  
3D Plot  
DIR  
Exits the Program

F2 key \*\*\*\*\*  
Monte Carlo  
Scattering  
Model

F3 key \*\*\*\*\*  
Brings the ANALYSIS MENU module  
and:  
Histogram  
Edge Operators  
Image Metrics  
2D PSD  
Filter PSD  
Signal Proc.  
Exits the Program

F4 key \*\*\*\*\*  
Cloud Structure Model  
--NOT CURRENTLY IMPLEMENTED

F5 key \*\*\*\*\*  
Brings the MODELING MENU module  
and:  
Monte Carlo  
Structure Model  
LOWIN  
LOWTRAN 6.1  
LOWPLT  
DIR  
Exits the Program  
and returns to DOS

F6 key \*\*\*\*\*  
LOWIN  
  
See the PC-TRAN manual [Ref.23]  
and the Lowtran-6 manual [Ref.15]

F7 key \*\*\*\*\*  
LOWTRAN 6.1

See the PC-TRAN manual [Ref.23]  
and Lowtran-6 Manual [Ref.15]

F8 key \*\*\*\*\*  
LOWPLT

See the PC-TRAN manual [Ref.23]  
and Lowtran-6 Manual [Ref.15]

F9 key \*\*\*\*\*  
Allows the examination of a  
directory during program execution

F0 key \*\*\*\*\*  
Stops program execution  
and returns to DOS.

## ANALYSIS MODULE

F1 key \*\*\*\*\*  
Brings the DISPLAY MENU model  
and:  
Data Select  
Cursor  
Threshold Image  
2D Plot  
3D Plot  
DIR  
Exit Program

F2 key \*\*\*\*\*  
Histograms the  
cloud image.

F3 key \*\*\*\*\*  
Brings the ANALYSIS MENU model  
and:  
Histogram  
Edge Operators  
Image Metrics  
2D PSD  
Filter PSD  
Signal Proc.  
Exit Program

F4 key \*\*\*\*\*  
Calculates  
metrics for the  
cloud image.  
  
NOT CURRENTLY  
IMPLEMENTED !

F5 key \*\*\*\*\*  
Brings the MODELLING MENU  
  
Monte Carlo  
Structure Model  
LOWIN  
LOWTRAN 6.1  
LOWPLT  
DIR  
Exit Program

F6 key \*\*\*\*\*  
Edge Operators  
  
NOT CURRENTLY  
IMPLEMENTED !

F7 key \*\*\*\*\*

Calculates and  
displays the  
2D Power  
Spectral density

F8 key \*\*\*\*\*

Performs 2D  
filtering on  
the cloud image  
and displays  
the results.

F9 key \*\*\*\*\*

Signal Process

NOT CURRENTLY  
IMPLEMENTED !

F0 key \*\*\*\*\*

Stops program  
execution and  
returns to DOS.

## APPENDIX D

### COMPUTER CODE SUPPLIED BY ONTAR COMPANY TO READ THE BEDFORD DATA FILES FROM THE BMAP CODE

```
integer*2 data(371,16),i2
character*1 head(128),filenm(65),c1(2),chsv
integer*2 openfh,rdmem,closfh,ier,nfh
equivalence (c1,i2)

c
1  write(6,*) ' Input Filename:'
    call gasciz(filenm)
    ier=openfh(0, filenm, nfh)
    if(ier .eq. 0) go to 2
    write(6,*) ' File error #', ier
    go to 1
2  write(6,*) ' '
c
c    read image
c    read two headers
c

    ibuf=iaddrs(head)
    ier=rdmem(nfh,ibuf,128)
    if(ier .ne. 0) go to 798
    write(*,30) (head(i) , i=1,128)
30  format (1x,64a1/1x,64a1)

    ier=rdmem(nfh,ibuf,128)
```

```

        if(ier .ne. 0) go to 798
        write(*,30) (head(i) , i=1,128)
        ibuf=iaddrs(data)
c       read data
        do 100 i=1,16
            ier=rdmen(nfh,ibuf,742)
            if(ier .ne. 0) go to 798
c
c       byte reverse
c
        do 101 j=1,371
            i2=data(j,i)
            chsv=c1(1)
            c1 (1)=c1 (2)
            c1 (2)=chsv
            data(j,i)=i2
101      continue
            ibuf=ibuf+742
100      continue
c
c       write data to screen
c
200     write(6,*)   Input channel # 1-16, 0 to Exit '
            read (5,*) ichan
            i = ichan
            if( i .eq. 0) stop

```

```

        if(i .lt. 1 .or. i .gt. 16) goto 200
        write(6,*) ' Channel #      ',i
        write(6,*) (data(j,i),j=1,371)
        write(6,*) ' '
        goto 200
        stop

```

c

c

```

798      write(6,*) ' read error #',ier
        stop
        end

```

```

subroutine gasciz(name)

```

c

```

character*1 name(65)

```

c

```

        read(5,1000) (name(i) , i=1,65)
1000     format(65a1)
        do 100 i=1,64
        if(name(i) .eq. ' ') go to 1
100      continue
        i=65
1       name(i)=char(0)
        return
        end

```



## LIST OF REFERENCES

1. Lloyd, J.M., Thermal Imaging Systems, pp. 18-66, Plenum Press, 1975.
2. Hudson, Richard Jr., Infrared system Engineering, pp. 1-60, 104-109, 557, John Wiley & Sons Inc., 1969.
3. Khalil Seyrafi, Electro Optical System Analysis, pp. 127-143, 234-237, Electro-optical Research Company, 1985.
4. Cooper, Alfred, Class Notes for PH 4253 Sensors Systems and Signals, Naval Postgraduate School, Monterey, CA, 1982.
5. Wolfe, William L. and Zissis, George J., The Infrared Handbook, pp. 3-105 to 3-109, Office of Naval Research, Department of the Navy, 1966.
6. Jamieson, John A., McFee, Raymond H., Plass, Gilbert, N., Grube, Robert, H. and Richards, Roberts C., Infrared Physics and Engineering, McGraw-Hill Book Company, 1963.
7. Dainty J.C., and Shaw R., Image Science-Principles Analysis and Evaluation of Photographic-Type Imaging Process, Academic Press, London, 1974.
8. Blackman B. and Tukey J.W., The Measurements Of Power Spectra, Dover Publications, Inc, New York, 1979.
9. Bell, E.E., Eisner, L., Young, J. and Oetjen, R.A.  
"Spectral Radiance of Sky and Terrain at Wavelengths 1 and 20 microns. II Sky Measurements", Journal of the

- Optical Society of America, Vol. 50, pp. 1313-1320, Dec. 1960.
10. McCartney, E.J., "Scattering by Molecules and Particles" Optics of the Atmosphere, John Wiley and Sons, New York, 1976.
  11. Feigelson E.M., Radiation in a Cloudy Atmosphere, pp. 221-225, D. Reidel Publishing Company, Dordrecht/Boston, 1984.
  12. Cox, C. and Munk, W., Bulletin of the Scripps Institution of Oceanography, pp. 401-488, Vol. 6, 1956.
  13. Kessler, B.V., "The Navy Background Measurements and Analysis Program (BMAP), Proceedings of the Second Tri-Service Cloud Modeling Workshop, NSWC, White Oaks, MD, June, 1984.
  14. Steinberg, R., Hirschman, A., and Blumethal, A., "Navy Infrared Backgrounds Measurement and Analysis Program-Test Plan," NRL Memorandum Report, Naval Research Laboratory, Washington, DC, 1983.
  15. Kneizys, F.X., Shettle, E.P., Gallery, W.O., Chetwynd, Jr., J.H., Abreu, L.W., Selby, J.E.A., Clough, S.A., and Fenn, R.W., "Atmospheric Transmittance/Radiance: Computer Code Lowtran 6," AFGL-TR-83-0187, Air Force Geophysics Laboratory, Hansom AFB, MA 01731, Aug. 1983.
  16. "NSWC clutter model code operators manual and program description document" Infrared Cloud/Sea Modeling and underlying Fundamental Physics, Ontar Corporation.

17. Meador, W.E. and Weaver, W.R., "Two Stream Approximations to Radiative Transfer in Planetary Atmospheres: A Unified Description of Existing Methods and a New Improvement," J. Atmosph. Sci. 37 630, 1980.
18. Young, S.J., "Scattering of Solar Radiation by Clouds," The Aerospace Corporation Report TR-0079 (4970-40)-1, December 1978.
19. Liou, Juo-Nan and Wittman, Gerald D., "Parameterization of the Radiative Properties of Clouds," J. Atmosph. Sci., 36, 1261, 1979.
20. Henyey, L.G. and Greenstein, J.L., Diffuse Radiation in the Galaxy, Astrophysics Journal, 93, 70, 1941.
21. Zachor, A.S., Holtzegr, J.A., and Smith, F.G. "I.R. Signature Study" Honeywell Electro-Optics Center, Report AFAL-TR-79-1012, February 1979.
22. Description of the Electronics Processing Equipment for the IRST Program, General Electric Company, Syracuse New-York, 6 May 1977.
23. PC-TRAN manual, ONTAR corporation, Brookline, MA 02146.
24. William Brent Lander, An Implementation of the Standard Image Transfer for Handling Absryl Data, Report AFAL.
25. Bohner Manfred, "A Tape Format for Transferral of image Data and Source Programs", Computer Graphics and Image Processing 11, Karlsruhe FRG, Feb. 1979. \_
26. Longmire, "A Final Technical Report on Calibration and

Use of Clutter Data for Simulation," Western Kentucky University, Bowling Green, KY 42101.

27. AGA Thermovision 780 Operating Manual, publication No 556 556 492 Ed 11, AGA Infrared systems AB, 1980.
28. AGEMA Infrared Systems, DISCO 3.0 Operating Manual, publication Pharos Company, AGEMA, 1 July 1985.

## INITIAL DISTRIBUTION LIST

	No. Copies
1. Defence Technical Information Center Cameron Station Alexandria, Virginia 22304-6145	2
2. Library, Code 0142 Naval Postgraduate School Monterey, California 93943-5002	2
3. Department Chairman, Code 61 Department of Physics Naval Postgraduate School Monterey, California 93943	1
4. Prof. A.W. Cooper, Code 61 Cr Department of Physics Naval Postgraduate School Monterey, California 93943	3
5. Prof. J.P. Powers Department of Electrical and Computer Engineering Naval Postgraduate School Monterey, California 93943	2

6. Hellenic Navy General Staff 4  
GEN / B2  
Stratopedo Papagou  
Hollargos  
Athens, GREECE
7. Commander, NAVSEASYSKOM 1  
ATTN. CDR B. W. CARVER, SEA 06W1-4  
Washington, DC 20362-5102
8. Commander, Naval Surface Weapons Center 1  
White Oaks Laboratory  
ATTN. Dr. B. V. Kessler, R42  
Silver Spring MD 20903-5000
9. Apostolos Kotsis 5  
Anatolikos Romylias 27  
Papagos  
Athens, 15669 GREECE

END

DATE

FILMED

DTIC

11-88